Sensor Fault Tolerant Control for a 3-DOF Helicopter Considering Detectability Loss

Xianghua Wang, *Member, IEEE,* Youqing Wang, *Senior Member, IEEE,* Ziye Zhang, Xiangrong Wang, *Senior Member, IEEE,* Ron Patton, *Fellow, IEEE*

***Abstract*—This paper proposes a novel active fault tolerant control (FTC) scheme for a 3-degree-of-freedom (3-DOF) helicopter with sensor faults. As a challenge, only attitude angles are considered available, so that when the sensors measuring the elevation/travel angles are faulty, the system with respect to the remaining healthy outputs is not detectable. To circumvent this issue, a new interval observer (IO) with adaptive parameters is formulated, providing good estimates of both disturbances and unmeasurable states. This IO acts not only as a state estimator for nominal controller but also as a fault detection and isolation (FDI) observer for the fault occurrence and location. After the fault location is determined, two different fault estimation (FE) schemes are developed according to whether or not the system is detectable. Using the fault estimates, a fault tolerant controller is constructed to ensure the acceptable performance of the faulty system. Finally, experiments on the 3-DOF helicopter platform are conducted to verify the effectiveness of the proposed scheme.**

***Index Terms*—Fault tolerant control, fault detection and isolation, fault estimation, 3-DOF helicopter.**

I. Introduction

Helicopters have a wide range of applications in military and civil fields due to their distinctive advantages in hovering, vertical take-off and landing [1]. However, as a helicopter is an unstable and nonlinear system that does not have actuator and sensor redundancy [1], any fault or failure in the helicopter system may result in catastrophic damage. Fault tolerant control (FTC), which is aimed to make the system tolerant to faults, is a good alternative. Two ways of FTC are distinguished, termed passive and active FTC [2]. In the passive FTC, a baseline controller is designed to ensure acceptable system performance for several possible fault scenarios; this may produce a conservative and over-designed controller as all possible fault scenarios rarely occur at the same time, and the occurrence of a fault that is not in the considered scenarios may cause instability. On the other hand, active FTC consists of a fault detection and isolation (FDI) unit for fault occurrence and location, and a fault estimation (FE) unit for fault magnitude and shape. All these fault information is used to reconfigure the parameters and/or structure of the controller. In this paper, an active FTC scheme will be developed for a 3-DOF helicopter.

FTC design for helicopter systems has been a hot research topic in recent years. The 3-DOF helicopter under consideration is a laboratory experiment that is often used in control research and education for the design and implementation of (non)linear control concepts [3]. Although some studies of FTC applied to the 3-DOF laboratory helicopter are available, most only consider actuator faults [4, 5]. In actual flight, sensor faults happen more frequently than actuator faults [6]. When sensor faults occur, the inaccurate output information is fed back into the controller, which then generates the wrong command, resulting in compromised stability [7]. In this case, the helicopter may oscillate violently, and fail to complete the task, or even crash.

There are few studies on sensor FTC of the 3-DOF laboratory helicopter. In [3], a robust controller for a 3-DOF helicopter was proposed in presence of actuator and sensor faults, whereas not only attitude angle but also angular velocity were assumed to be measurable. It should be noted that the three attitude angles are measured by different encoders mounted on the instrumented joints in the 3-DOF laboratory helicopter; whereas there are no sensors directly measuring angular velocity information [8]. A hierarchical structure-based sensor fault-tolerant consensus protocol was proposed for multiple 3-DOF helicopters using only attitude angle measurement in [9] and [10], where there was no FDI unit for the fault location, and instead an FE unit was utilized. Since the fault location is unknown, it is conservatively assumed that faults could happen in all components and the FE unit which is activated at the beginning of system operation needs to estimate all these faults. Thus, the schemes in [9, 10] are largely conservative and moreover, need more available information for the estimation of all faults. Therefore, it is challenging to develop sensor active FTC for a 3-DOF laboratory helicopter when only attitude angles can be directly measured.

FDI/FE units are typically observer-based [11, 12], and the interval observer (IO), consisting of a pair of Luenberger observers that give the upper/lower bounds of the state [13], is a popular choice. Current works on IOs [13, 14] use the constant disturbance bounds as observer parameters, and when the disturbance bounds are conservative, a large interval length defined as the difference between the upper and lower bounds will be resulted in. Therefore, when applied to the

X. Wang is with the School of Artificial Intelligence, Beijing University of Posts and Telecommunications, Beijing, China, XianghuaWang@bupt.edu.cn. The corresponding author.

Y. Wang is with the College of Information Science and Technology, Beijing University of Chemical Technology, Beijing, China, wang.youqing@ieee.org

Z. Zhang is with the College of Mathematics and Systems Science, Shandong University of Science and Technology, Qingdao, China, zhangzy02@126.com

X. Wang is with the School of Electronic and Information Engineering, Beihang University, Beijing, China, xrwang@buaa.edu.cn

R. Patton is with the School of Engineering, University of Hull, UK, R.J.Patton@hull.ac.uk

fault detection [15], it will generate large fault missing/false alarm rates. In addition, for the IO to estimate unknown inputs, it needs high-order derivatives of outputs [16], which in turn requires the outputs to be sufficiently smooth with bounded derivatives; however, in real systems such as the helicopter, this condition might not be satisfied.

In this paper, an active FTC for a 3-DOF laboratory helicopter with sensor faults is investigated when only attitude angles are measurable. Firstly, a novel IO is designed for the fault occurrence and location. According to the fault location, the system detectability with respect to the remaining healthy outputs will be determined, from which two different FE schemes are developed. Using the fault estimate, fault tolerant controller is established to ensure the acceptable performance of the faulty system. The novelties and contributions compared to the existing works can be summarized as:

- Unlike the existing IO where the bounds of disturbances are used as observer parameters [17], the proposed adaptive IO utilizes adaptive parameters instead. Hence tighter bounds of states and disturbances are yielded.
- Different from established FDI schemes which require either a set of dissimilar observers or dissimilar residual signals [18], the fault occurrence and location are simultaneously obtained by only one proposed adaptive IO, not only reducing the computational cost but also shortening the fault diagnosis time.
- When the system detectability with respect to the remaining healthy outputs is lost due to a fault occurring in some sensor, the existing FE methods [9] and [10] are not applicable, and a novel FE scheme based on sliding mode equivalent output injection and Volterra integral equation (VIE) is proposed to obtain the fault estimate.

This paper is organized as follows. In Section II, helicopter dynamics, problem formulation and preliminaries are presented. In Section III, nominal controller and FDI based on a novel IO are designed. FE and FTC schemes are developed in Section IV. Experiments are given in Section V and conclusions are drawn in Section VI.

Notations: in this paper, $\mathbf{I}_r$ is an identity matrix of dimension r, $\mathbf{1}_r$ is a column vector of size r and all its entries are 1. $\mathbf{0}$ is a matrix or vector with appropriate dimension and its all entries are 0. For a real matrix $X \in \mathbb{R}^{n\times m}$, $\text{row}(X)_i$ is the ith row of X, $X(i,j)$ is the element of X in the ith row and jth column, $X_r = \left[\begin{array}{c:c:c} \mathbf{I}_{i-1} & \mathbf{0} & \mathbf{0} \\ \mathbf{0} & \mathbf{0} & \mathbf{I}_{n-i} \end{array}\right] X$, namely the remaining part of X with its ith row removed, $X^+(i,j) = \max\{0, X(i,j)\}$ and $X^- = X^+ - X$, $|X| = X^+ + X^-$. A real matrix X is known as Metzler if all its off-diagonal entries are nonnegative ($X(i,j) \geq 0, i \neq j$) [17]. For a symmetric positive definite (s.p.d.) matrix P, the minimum and maximum eigenvalues of P are denoted respectively as $\lambda_{min}(P)$ and $\lambda_{max}(P)$. For a vector x, $\|x\| = \sqrt{x^T x}$; the upper and lower bounds of x are denoted as $\overline{x}$ and $\underline{x}$ respectively, namely $\underline{x} \preceq x \preceq \overline{x}$. For vectors a and b, $a \preceq (\succeq) b$ means $\forall i : a_i \leq (\geq) b_i$; define $c_{max} = \max\{a,b\} \triangleq \text{col}[\max\{a_i, b_i\}]$ and $c_{min} = \min\{a,b\} \triangleq \text{col}[\min\{a_i, b_i\}]$ where $\text{col}[x_i]$ is a column vetor whose ith component is x_i, then $c_{max} \succeq a$, $c_{max} \succeq b$, $c_{min} \preceq a$ and $c_{min} \preceq b$.

II. Problem Formulation and Preliminaries

In this section, the dynamics of a 3-DOF laboratory helicopter is first presented, and then problem formulation and some Lemmas needed to derive the main results are given.

A. Helicopter dynamics

The free-body diagram of a 3-DOF helicopter is shown in Fig. 1. Let ε, ρ, λ be the elevation, pitch and travel angles (in degrees), respectively, and $\varepsilon_d, \rho_d, \lambda_d$ be the corresponding desired constant values. V_f and V_b are control voltages of the front and back motors (in volts), which generate the thrust F_f and F_b.

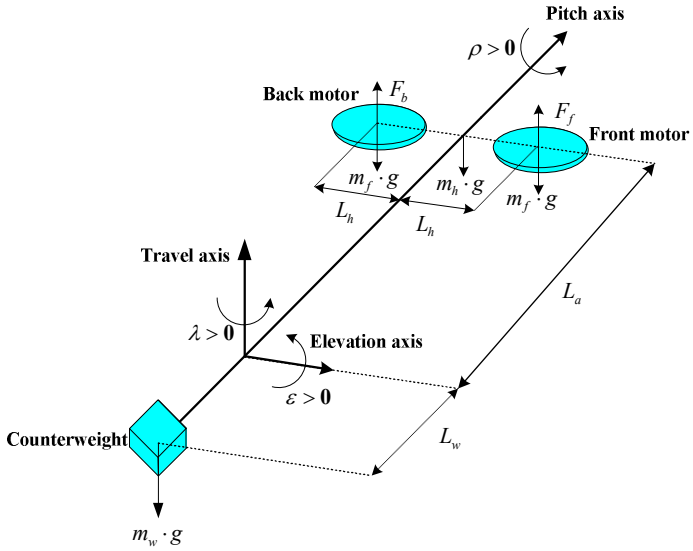

Fig. 1: Free-body diagram of a 3-DOF helicopter.

Using the Euler-Lagrange formula, the nonlinear equations of motion of the 3-DOF helicopter system are derived as [19]

$$\begin{array}{rcl} J_e\ddot{\varepsilon} & = & K_f(V_f+V_b)L_a\cos(\rho) - T_g\cos(\varepsilon) \\ J_t\ddot{\lambda} & = & -T_g\sin(\rho) \\ J_\rho\ddot{\rho} & = & K_f(V_f-V_b)L_h \end{array} \tag{1}$$

where $J_e = 2m_fL_a^2 + m_wL_w^2$, $J_e = 2m_f(L_a^2+L_h^2) + m_wL_w^2$, $J_\rho = 2m_fL_h^2$, $T_g = g(m_wL_w - 2m_fL_a)$. Considering the effect of counterweight, quiescent voltage of both front and back motor is used to balance the equivalent weight of the helicopter platform as $V_{op} = T_g/(2L_aK_f)$. Define the state, input and output vectors as $x^T = [\varepsilon - \varepsilon_d, \rho - \rho_d, \lambda - \lambda_d, \dot{\varepsilon} - \dot{\varepsilon}_d, \dot{\rho} - \dot{\rho}_d, \dot{\lambda} - \dot{\lambda}_d]$, $u^T = [V_f - V_{op}, V_b - V_{op}]$ and $y^T = [\varepsilon - \varepsilon_d, \rho - \rho_d, \lambda - \lambda_d]$. Linearize the nonlinear model (1) about zero and approximate $\sin(\rho) \approx \rho$, $\cos(\rho) \approx 1$ and $\cos(\varepsilon) \approx 1$. Thus, the linear state-space model of a 3-DOF helicopter can be described as

$$\dot{x} = Ax + Bu + Dd,\ y = Cx \tag{2}$$

where the state-space matrices are $C = [\mathbf{I}_3\ \mathbf{0}]$,

$$\begin{array}{l} A = \left[\begin{array}{c:c} \mathbf{0} & \mathbf{I}_3 \\ \hline A^0 & \mathbf{0} \end{array}\right], A^0 = \left[\begin{array}{ccc} 0 & 0 & 0 \\ 0 & 0 & 0 \\ 0 & a_{32} & 0 \end{array}\right], \\ B = \left[\begin{array}{c} \mathbf{0} \\ \hline B^0 \end{array}\right], B^0 = \left[\begin{array}{cc} b_{11} & b_{11} \\ b_{22} & -b_{22} \\ 0 & 0 \end{array}\right] \end{array} \tag{3}$$

where $a_{32} = -\frac{(L_w m_w - 2L_a m_f)g}{J_t}$, $b_{11} = \frac{L_a K_f}{J_e}$, $b_{22} = \frac{K_f L_h}{J_p}$. The values of model parameters in (3) are given in Table I. d is the external disturbance which can be generated by an active disturbance system (ADS) equipped on the arm of the lab helicopter [8]. Actually, the ADS exerts extra moments acting in the angular velocity channels as disturbances, hence the disturbance distribution matrix D is given by $D = [\mathbf{0}\ \mathbf{I}_3]^T$. It should be noted that the 3-DOF laboratory helicopter does not equip the individual sensors to measure the angular velocities [8]. In the following, we denote the size of x, u, d and y as n, m, q and p, respectively.

Suppose the ith sensor is experiencing an additive fault, then the output equation is not $y = Cx$ but

$$y = Cx + E_i f_{s,i} \tag{4}$$

where $E_i \in \mathbb{R}^{p\times 1}$ with its ith entry being 1 and others being 0. Similar to [20], the fault $f_{s,i}$ has the form of

$$f_{s,i} = \beta_i(t) f^*_{s,i}(t) \tag{5}$$

where $f^*_{s,i}(t)$ and $\dot{f}^*_{s,i}(t)$ are assumed to be bounded, and

$$\beta_i(t) = \begin{cases} 0, & 0 \le t < T_F \\ 1 - e^{-\alpha(t-T_F)}, & t \ge T_F \end{cases}, \tag{6}$$

where the scalar α denotes the unknown fault-evolution rate. $T_F > 0$ denotes the unknown fault-occurrence time.

Remark 1: Differentiate $\beta_i(t)$ in (6) once to get

$$\dot{\beta}_i(t) = \begin{cases} 0, & 0 \le t < T_F \\ \infty, & t = T_F \\ 0 < \alpha e^{-\alpha(t-T_F)} < \alpha, & t > T_F \end{cases} \tag{7}$$

From $\dot{f}_{s,i} = \dot{\beta}_i f^*_{s,i} + \beta_i \dot{f}^*_{s,i}$, it is obvious that $\dot{f}_{s,i}(T_F) = \infty$ and $\dot{f}_{s,i}(t) < \infty$ for $t > T_F$, namely $\dot{f}_{s,i}$ is not continuous at $t = T_F$ and has a pulse change.

Remark 2: When the ith sensor is experiencing a multiplicative fault. the output equation can also be written as (4) and (5) where $f^*_{s,i} = -\rho_i \mathrm{row}(C)_i x$ with $0 < \rho_i < 1$ being the efficiency loss coefficient.

Divide y in (4) into $y \mapsto \begin{bmatrix} y_f^T & y_r^T \end{bmatrix}^T$ where

$$y_f = \mathrm{row}(C)_i x + f_{s,i}, y_r = C_r x \tag{8}$$

where $\mathrm{row}(C)_i$ and C_r are defined in Notations. Observing (3) and (8), it can be found that

(a) C has full row rank, B and D have full column rank;
(b) A is not Hurwitz;
(c) (A,B) is controllable, and (A,C) is observable;
(d) $\mathrm{rank}(CD) \neq \mathrm{rank}(D)$;
(e) the triple (A,D,C) is minimum phase;
(f) the couple (A,C_r) is not detectable when the 1st or 3rd sensor measuring the elevation/travel angle has a fault;
(g) There does not exist a matrix N such that $D = BN$, namely the disturbance d is unmatched.

Remark 3: From the discussion above, it is known that for the 3-DOF helicopter system (2), A is not Hurwitz and (A,C_r) is not detectable when the 1st or 3rd sensor measuring the elevation/travel angle is faulty, which brings difficulties in the design of observer-based FDI and FE.

TABLE I: Model parameters [19]

Parameter	Value	Unit	Description
K_f	0.1188	N/V	Propeller force-thrust constant
m_f	0.575	kg	Mass of the front- and back-propeller assembly
m_h	1.15	kg	Mass of the helicopter
m_w	1.87	kg	Mass of the counterweight
L_a	0.6604	m	Distance between the travel axis and the helicopter
L_h	0.1778	m	Distance between the pitch axis and each motor
L_w	0.4600	m	Distance between the travel axis and the counter-weight
g	9.8	$m \cdot s^2$	Gravity constant

B. Problem Formulation

Assumption 1: The disturbance d is constant and unknown, but its upper/lower bounds $\overline{d}^c/\underline{d}^c$ are known and conservative, which is a general situation since it is difficult to get accurate bounds.

Assumption 2: The initial state $x(0)$ is unknown but bounded by $\underline{x}_0^c \preceq x(0) \preceq \overline{x}_0^c$, where $\underline{x}_0^c$ and $\overline{x}_0^c$ are available and conservative.

Assumption 3: Only one fault might occur at any one time, which is reasonable since in practice, it is highly unlikely that two or more sensor faults occur simultaneously.

Remark 4: Since wind can affect position and trajectory tracking, it is the main external disturbance for a 3-DOF helicopter and can be regarded as a hybrid model of a static dominant constant and a wind gust which is a periodic signal [21]. In this work, only the static dominant constant of wind is considered, hence in Assumption 1, the disturbance d is assumed to be constant and bounded.

The goal is to design an output feedback based active FTC scheme, as shown in Fig.2, such that

$$\|x\| \le \gamma_s \|d\| \tag{9}$$

can be ensured when some sensor is faulty, where $\gamma_s > 0$ denotes the acceptable level of system performance.

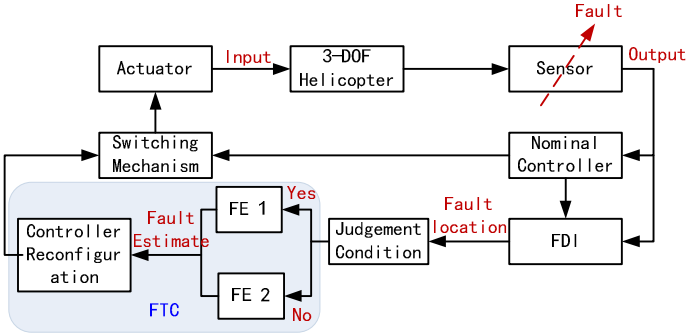

Fig. 2: The block diagram of the proposed active FTC scheme.

C. Preliminaries

Here we present Lemmas needed to derive the main results.

Lemma 1: [17] For a matrix A and a vector x with $\underline{x} \preceq x \preceq \overline{x}$, it follows that $A^+\underline{x} - A^-\overline{x} \preceq Ax \preceq A^+\overline{x} - A^-\underline{x}$.

Lemma 2: [22] For a non-autonomous system $\dot{x}(t) = Ax(t) + g(t)$, where A is Metzler and $g(t) \succeq \mathbf{0}, \forall t \geq 0$. If $x(0) \succeq \mathbf{0}$, then it follows that $x(t) \succeq \mathbf{0}$ for all $t \geq 0$.

Proposition 1: For a system $\dot{e} = A_e e + D_e d_e$ where A_e is Hurwitz and hence there exist s.p.d. matrices P_e and Q_e such that $A_e^T P_e + P_e A_e = -Q_e$, d_e is a bounded disturbance, then for $t \geq 0$, $\min\left\{\frac{2\|P_eD_e\|\|d_e\|\sqrt{\lambda_{max}(P_e)}}{\sqrt{\lambda_{min}(P_e)}\lambda_{min}(Q_e)}, \|e(0)\|\right\} \leq \|e(t)\| \leq \max\left\{\frac{2\|P_eD_e\|\|d_e\|\sqrt{\lambda_{max}(P_e)}}{\sqrt{\lambda_{min}(P_e)}\lambda_{min}(Q_e)}, \|e(0)\|\right\}$ and as $t \to \infty$, $\|e(t)\| \to \frac{2\|P_eD_e\|\|d_e\|\sqrt{\lambda_{max}(P_e)}}{\sqrt{\lambda_{min}(P_e)}\lambda_{min}(Q_e)}$ with $e(0)$ being the initial state.

Proof: Define the Lyapunov function $V_e = 0.5e^T P_e e$ and differentiate V_e once to get

$$\begin{aligned} \dot{V}_e &= -0.5e^T Q_e e + e^T P_e D_e d_e \\ &\leq -0.5\lambda_{min}(Q_e)\|e\|^2 + \|e\|\|P_eD_e\|\|d_e\| \end{aligned} \tag{10}$$

Using $0.5\lambda_{min}(P_e)\|e\|^2 \leq V_e \leq 0.5\lambda_{max}(P_e)\|e\|^2$, it further follows that

$$\dot{V}_e \leq -\frac{\lambda_{min}(Q_e)}{\lambda_{max}(P_e)}V_e + \frac{\sqrt{2}\|P_eD_e\|\|d_e\|}{\sqrt{\lambda_{min}(P_e)}}\sqrt{V_e} \tag{11}$$

Denote $W_e = \sqrt{V_e}$ and $k_w = \lambda_{min}(Q_e)/(2\lambda_{max}(P_e))$, and from (11) it follows

$$\dot{W}_e \leq -k_w W_e + \frac{\sqrt{2}\|P_eD_e\|\|d_e\|}{2\sqrt{\lambda_{min}(P_e)}} \tag{12}$$

which is solved to get

$$W_e(t) \leq \left(W_e(0) - \frac{\sqrt{2}\|P_eD_e\|\|d_e\|}{2k_w\sqrt{\lambda_{min}(P_e)}}\right)e^{-k_w t} + \frac{\sqrt{2}\|P_eD_e\|\|d_e\|}{2k_w\sqrt{\lambda_{min}(P_e)}}$$

It follows that for $t \geq 0$,

$$\begin{aligned} &\min\left\{\frac{\sqrt{2}\|P_eD_e\|\|d_e\|}{2k_w\sqrt{\lambda_{min}(P_e)}}, W_e(0)\right\} \leq W_e(t) \\ &\leq \max\left\{\frac{\sqrt{2}\|P_eD_e\|\|d_e\|}{2k_w\sqrt{\lambda_{min}(P_e)}}, W_e(0)\right\} \end{aligned} \tag{13}$$

and as $t \to \infty$, $W_e(t) \to \frac{\sqrt{2}\|P_eD_e\|\|d_e\|}{2k_w\sqrt{\lambda_{min}(P_e)}}$. Hence

$$\begin{aligned} &\min\left\{\frac{2\|P_eD_e\|\|d_e\|\sqrt{\lambda_{max}(P_e)}}{\sqrt{\lambda_{min}(P_e)}\lambda_{min}(Q_e)}, \|e(0)\|\right\} \leq \|e(t)\| \\ &\leq \max\left\{\frac{2\|P_eD_e\|\|d_e\|\sqrt{\lambda_{max}(P_e)}}{\sqrt{\lambda_{min}(P_e)}\lambda_{min}(Q_e)}, \|e(0)\|\right\} \end{aligned} \tag{14}$$

and as $t \to \infty$, $\|e(t)\| \to \frac{2\|P_eD_e\|\|d_e\|\sqrt{\lambda_{max}(P_e)}}{\sqrt{\lambda_{min}(P_e)}\lambda_{min}(Q_e)}$. ■

III. Fault Detection and Isolation

In this section, a novel interval observer (IO) is first proposed to obtain the estimates of both disturbance and unmeasurable states. A nominal controller and a fault detection and isolation (FDI) unit based on the novel IO are then developed.

A. Novel interval observer

For the 3-DOF helicopter model (3), there exists a state transformation $x \mapsto T_0 x$ with $T_0 = \begin{bmatrix} \mathbf{0} & \mathbf{I}_3 \\ \mathbf{I}_3 & \mathbf{0} \end{bmatrix}$ such that

$$\begin{aligned} &T_0 A T_0^{-1} \mapsto \left[\begin{array}{c|c} A_1^{**} & A_2^{**} \\ \hline A_3^{**} & A_4^{**} \end{array}\right], T_0 D \mapsto \left[\begin{array}{c} D_1^{**} \\ \hline D_2^{**} \end{array}\right], \\ &CT_0^{-1} \mapsto \left[\begin{array}{c|c} \mathbf{0} & C^{**} \end{array}\right] \end{aligned} \tag{15}$$

where $C^{**} \in \mathbb{R}^{p\times p}$ is an invertible matrix. From the fact that the pair (A,C) is observable and the structures in (15), it is apparent that the couple (A_1^{**}, A_3^{**}) is observable. Hence there exists a matrix $L^* \in \mathbb{R}^{(n-p)\times p}$ such that the eigenvalues of $A_1^* = A_1^{**} + L^* A_3^{**}$ denoted as $\lambda_1, \cdots, \lambda_{n-p}$ satisfy

$$\lambda_i \approx \lambda \text{ and } \lambda_i \neq \lambda_j (i \neq j) \tag{16}$$

where $\lambda < 0$ is a design scalar given later in Remark 6 and Remark 15. Establish another transformation $x \mapsto T_1 T_0 x$ where $T_1 = \begin{bmatrix} \mathbf{I}_{n-p} & L^* \\ \mathbf{0} & C^{**} \end{bmatrix}$, then $CT_0^{-1}T_1^{-1} \mapsto \left[\begin{array}{c|c} \mathbf{0} & \mathbf{I}_p \end{array}\right]$,

$$T_1 T_0 A T_0^{-1} T_1^{-1} \mapsto \left[\begin{array}{c|c} A_1^* & A_2^* \\ \hline A_3^* & A_4^* \end{array}\right], T_1 T_0 D \mapsto \left[\begin{array}{c} D_1^* \\ \hline D_2^* \end{array}\right] \tag{17}$$

From (16), it is known that there exists a nonsingular matrix S such that $SA_1^*S^{-1} = A_1$ where

$$A_1 = \text{diag}\{\lambda_1, \cdots, \lambda_{n-p}\} \approx \Lambda = \text{diag}\{\lambda\}. \tag{18}$$

Introduce a nonsingular transformation $x \mapsto \underbrace{T_2 T_1 T_0}_{T} x$ with $T_2 = \begin{bmatrix} S & \mathbf{0} \\ \mathbf{0} & \mathbf{I}_p \end{bmatrix}$, then $CT^{-1} \mapsto \left[\begin{array}{c|c} \mathbf{0} & \mathbf{I}_p \end{array}\right]$, $TB \mapsto \left[\begin{array}{c} B_1 \\ \hline B_2 \end{array}\right]$,

$$TAT^{-1} \mapsto \left[\begin{array}{c|c} A_1 & A_2 \\ \hline A_3 & A_4 \end{array}\right], TD \mapsto \left[\begin{array}{c} \bar{D}_1 \\ \hline \bar{D}_2 \end{array}\right] \tag{19}$$

Therefore, the system (2) is transformed and partitioned into

$$\dot{x}_1 = A_1 x_1 + A_2 x_2 + B_1 u + \bar{D}_1 d, \tag{20a}$$

$$\dot{x}_2 = A_3 x_1 + A_4 x_2 + B_2 u + \bar{D}_2 d \tag{20b}$$

when all sensors are healthy $y = x_2$, A_1 is from (18) and Hurwitz and Metzler.

Remark 5: From Assumption 2 and the transformation $x \mapsto Tx$, the bounds of $x_1(0)$ are $\underline{x}_{10}^c \preceq x_1(0) \preceq \overline{x}_{10}^c$, where $\underline{x}_{10}^c = [\mathbf{I}_{n-p}\ \mathbf{0}](T^+\underline{x}_0^c - T^-\overline{x}_0^c)$, $\overline{x}_{10}^c = [\mathbf{I}_{n-p}\ \mathbf{0}](T^+\overline{x}_0^c - T^-\underline{x}_0^c)$.

We propose the following observers for the system (20)

$$\dot{\hat{x}}_1 = A_1\hat{x}_1 + A_2 y + B_1 u, \tag{21}$$

$$\begin{aligned} \dot{\overline{x}}_2 &= \Gamma\overline{e}_y + A_3\hat{x}_1 + A_4 y + B_2 u + \overline{\delta} \\ \dot{\underline{x}}_2 &= -\Gamma\underline{e}_y + A_3\hat{x}_1 + A_4 y + B_2 u + \underline{\delta} \end{aligned} \tag{22}$$

where $\overline{e}_y = \overline{y} - y$, $\underline{e}_y = y - \underline{y}$, $\underline{y} = \underline{x}_2$, $\overline{y} = \overline{x}_2$. And $\overline{\delta} = [\overline{\delta}_1, \cdots, \overline{\delta}_p]$, $\underline{\delta} = [\underline{\delta}_1, \cdots, \underline{\delta}_p]$, $\underline{\delta}_i$, $\overline{\delta}_i, i = 1, \cdots, p$ are determined by the following adaptive laws:

$$\begin{aligned} \dot{\overline{\delta}}_i &= -k_\delta(\text{sgn}(\overline{e}_{y,i} - \varepsilon_{\delta,1}) + \text{sgn}(\overline{e}_{y,i} - \varepsilon_{\delta,2})) \\ \dot{\underline{\delta}}_i &= k_\delta(\text{sgn}(\underline{e}_{y,i} - \varepsilon_{\delta,1}) + \text{sgn}(\underline{e}_{y,i} - \varepsilon_{\delta,2})) \end{aligned} \tag{23}$$

where $\overline{e}_{y,i}$ and $\underline{e}_{y,i}$ are the i-th component of $\overline{e}_y$ and $\underline{e}_y$ respectively, and $\varepsilon_{\delta,1} > \varepsilon_{\delta,2} > 0$ are user-defined constants which determine the width of $\overline{e}_{y,i}$ and $\underline{e}_{y,i}$, and $k_\delta > 0$ is a

user-defined constant which determines the changing rates of $\overline{\delta}_i$ and $\underline{\delta}_i$. The choice of k_δ will be given in (64). $\hat{x}_1(0)$ is the initial value of $\hat{x}_1$ and can be arbitrary value. $\underline{\delta}_i(0)$ and $\overline{\delta}_i(0)$ are the initial values of $\underline{\delta}_i$ and $\overline{\delta}_i$ respectively, and also the i-th component of $\underline{\delta}(0)$ and $\overline{\delta}(0)$ respectively, chosen as

$$\begin{aligned}\underline{\delta}(0) &= \min\{\underline{\delta}^c, A_3^+\underline{x}_{10}^c - A_3^-\overline{x}_{10}^c - A_3\hat{x}_1(0) + \bar{D}_2^+\underline{d}^c - \bar{D}_2^-\overline{d}^c\}\\ \overline{\delta}(0) &= \max\{\overline{\delta}^c, A_3^+\overline{x}_{10}^c - A_3^-\underline{x}_{10}^c - A_3\hat{x}_1(0) + \bar{D}_2^+\overline{d}^c - \bar{D}_2^-\underline{d}^c\}\end{aligned} \tag{24}$$

where $\underline{\delta}^c$, $\overline{\delta}^c$ are given later in (29). $\overline{y}(0)(\overline{x}_2(0))$ and $\underline{y}(0)(\underline{x}_2(0))$ are the initial values of $\overline{y}(t)(\overline{x}_2(t))$ and $\underline{y}(t)(\underline{x}_2(t))$ respectively, chosen to satisfy $\overline{e}_y(0) \succ \varepsilon_{\delta,1}\mathbf{1}_p$ and $\underline{e}_y(0) \succ \varepsilon_{\delta,1}\mathbf{1}_p$. $\Gamma = \mathrm{diag}\{\gamma\}$ and $\gamma < 0$ is a scalar whose choice makes

$$\begin{aligned}&\overline{\delta}(0) - A_3^+\underline{x}_{10}^c + A_3^-\overline{x}_{10}^c + A_3\hat{x}_1(0) - \bar{D}_2^+\underline{d}^c + \bar{D}_2^-\overline{d}^c \prec -\gamma\varepsilon_{\delta,1}\mathbf{1}_p\\ &\bar{D}_2^+\overline{d}^c - \bar{D}_2^-\underline{d}^c - \underline{\delta}(0) + A_3^+\overline{x}_{10}^c - A_3^-\underline{x}_{10}^c - A_3\hat{x}_1(0) \prec -\gamma\varepsilon_{\delta,1}\mathbf{1}_p\end{aligned} \tag{25}$$

with $\overline{x}_{10}^c$ and $\underline{x}_{10}^c$ from Remark 5, and $\overline{d}^c$ and $\underline{d}^c$ from Assumption 1.

Denote $\tilde{x}_1 = x_1 - \hat{x}_1$, and subtract (21) from (20a) to get $\dot{\tilde{x}}_1 = A_1\tilde{x}_1 + \bar{D}_1 d$, which is solved to obtain

$$\tilde{x}_1(t) = e^{A_1 t}\tilde{x}_1(0) + e^{A_1 t}\int_0^t e^{-A_1\tau}d\tau\ \bar{D}_1 d \tag{26}$$

From (18), (26) can be approximated as

$$\begin{aligned}\tilde{x}_1(t) &\approx e^{\Lambda t}\tilde{x}_1(0) + e^{\Lambda t}\textstyle\int_0^t e^{-\Lambda\tau}d\tau\ \bar{D}_1 d\\ &= \underbrace{e^{\Lambda t}(\tilde{x}_1(0) + \Lambda^{-1}\bar{D}_1 d)}_{h_1} - \Lambda^{-1}\bar{D}_1 d\end{aligned} \tag{27}$$

From $\lambda < 0$ and Assumption 1, it follows that $h_1 \to \mathbf{0}$ as $t \to \infty$. Combine (20b) with (27) to get

$$\begin{aligned}\dot{x}_2 &= A_3\tilde{x}_1 + A_3\hat{x}_1 + A_4 x_2 + B_2 u + \bar{D}_2 d\\ &= A_3\hat{x}_1 + A_4 x_2 + B_2 u + A_3 h_1 + \delta\end{aligned} \tag{28}$$

where $\delta = D_2 d$, $D_2 = \bar{D}_2 - A_3\Lambda^{-1}\bar{D}_1$.

Remark 6: The choice of λ (the diagonal element of Λ) should make D_2 full of column rank.

Remark 7: From Assumption 1 and Lemma 1, the conservative bounds for δ are

$$\underline{\delta}^c \preceq \delta \preceq \overline{\delta}^c, \underline{\delta}^c = D_2^+\underline{d}^c - D_2^-\overline{d}^c, \overline{\delta}^c = D_2^+\overline{d}^c - D_2^-\underline{d}^c \tag{29}$$

Proposition 2: For the system (28), the proposed IO (22)-(23) can achieve $\overline{x}_2 - x_2 \succeq \varepsilon_{\delta,1}1_p$ and $x_2 - \underline{x}_2 \succeq \varepsilon_{\delta,1}1_p$ for $0 \le t \le T_s$; $\varepsilon_{\delta,2}1_p \prec \overline{x}_2 - x_2 \prec \varepsilon_{\delta,1}1_p$ and $\varepsilon_{\delta,2}1_p \prec x_2 - \underline{x}_2 \prec \varepsilon_{\delta,1}1_p$ for $t > T_s$, where T_s is a finite time.

Proof: When there are no sensor faults, $y = x_2$ and subtract (22) from (28) to get

$$\dot{\overline{e}}_y = \Gamma\overline{e}_y + \overline{\delta} - \delta - A_3 h_1, \dot{\underline{e}}_y = \Gamma\underline{e}_y + \delta - \underline{\delta} + A_3 h_1 \tag{30}$$

where

$$\begin{aligned}&\overline{\delta}(0) - \delta(0) - A_3 h_1(0)\\ =\ &\overline{\delta}(0) - D_2 d(0) - A_3(x_1(0) - \hat{x}_1(0) + \Lambda^{-1}\bar{D}_1 d(0))\\ =\ &\overline{\delta}(0) - A_3 x_1(0) + A_3\hat{x}_1(0) - \bar{D}_2 d(0)\end{aligned} \tag{31}$$

From Lemma 1, Assumption 1 and Remark 5, (31) can be further written as

$$l_1 \preceq \overline{\delta}(0) - \delta(0) - A_3 h_1(0) \preceq u_1 \tag{32}$$

where $l_1 = \overline{\delta}(0) - A_3^+\overline{x}_{10}^c + A_3^-\underline{x}_{10}^c + A_3\hat{x}_1(0) - \bar{D}_2^+\overline{d}^c + \bar{D}_2^-\underline{d}^c$, $u_1 = \overline{\delta}(0) - A_3^+\underline{x}_{10}^c + A_3^-\overline{x}_{10}^c + A_3\hat{x}_1(0) - \bar{D}_2^+\underline{d}^c + \bar{D}_2^-\overline{d}^c$. Using (24) and (25), (32) becomes

$$\mathbf{0} \preceq l_1 \preceq \overline{\delta}(0) - \delta(0) - A_3 h_1(0) \preceq u_1 \preceq -\gamma\varepsilon_{\delta,1}\mathbf{1}_p \tag{33}$$

Similarly, it follows $\mathbf{0} \preceq \delta(0) - \underline{\delta}(0) + A_3 h_1(0) \preceq -\gamma\varepsilon_{\delta,1}\mathbf{1}_p$. Moreover, from $\overline{e}_y(0) \succ \varepsilon_{\delta,1}\mathbf{1}_p$ and (33), it follows that

$$\begin{aligned}\dot{\overline{e}}_y(0) &= \Gamma\overline{e}_y(0) + \overline{\delta}(0) - \delta(0) - A_3 h_1(0)\\ &\prec \gamma\varepsilon_{\delta,1}\mathbf{1}_p - \gamma\varepsilon_{\delta,1}\mathbf{1}_p\\ &= \mathbf{0}\end{aligned} \tag{34}$$

Similarly, $\dot{\underline{e}}_y(0) \prec \mathbf{0}$ can be obtained. From $\overline{e}_y(0) \succ \varepsilon_{\delta,1}\mathbf{1}_p \succ \mathbf{0}$, $\dot{\overline{e}}_y(0) \prec \mathbf{0}$, $\overline{\delta}(0) - \delta(0) - A_3 h_1(0) \succeq \mathbf{0}$, and the continuity of $\overline{e}_y(t)$ with respect to t, it follows that there exists a period of time $[0, T_a)$ when $\overline{e}_y(t) \succ \mathbf{0}$, $\dot{\overline{e}}_y(t) \prec \mathbf{0}$, and $\dot{\overline{e}}_y(T_a) = \mathbf{0}$.

From (30), the dynamics of $\overline{e}_{y,i}$ and $\underline{e}_{y,i}$ are written as

$$\dot{\overline{e}}_{y,i} = \gamma\overline{e}_{y,i} + \overline{\delta}_i - \delta_i - \mathrm{row}(A_3)_i h_1 \tag{35}$$

$$\dot{\underline{e}}_{y,i} = \gamma\underline{e}_{y,i} + \delta_i - \underline{\delta}_i + \mathrm{row}(A_3)_i h_1 \tag{36}$$

Define $V_i = \frac{1}{2}\overline{e}_{y,i}^2$ which is differentiated once using (35) to get

$$\dot{V}_i = \gamma\overline{e}_{y,i}^2 + \overline{e}_{y,i}(\overline{\delta}_i - \delta_i - \mathrm{row}(A_3)_i h_1) \tag{37}$$

It is clear from (37) that when $\overline{e}_{y,i} > -\left(\overline{\delta}_i - \delta_i - \mathrm{row}(A_3)_i h_1\right)/\gamma$, $\dot{V}_i < 0$. Hence the set $\Psi = \left\{\overline{e}_{y,i}(t) \le -(\overline{\delta}_i(t) - \delta_i(t) - \mathrm{row}(A_3)_i h_1(t))/\gamma\right\}$ is an invariant set. Since $\dot{\overline{e}}_{y,i}(T_a) = 0$, from (35), it follows that

$$\overline{e}_{y,i}(T_a) = -(\overline{\delta}_i(T_a) - \delta_i(T_a) - \mathrm{row}(A_3)_i h_1(T_a))/\gamma \tag{38}$$

hence the trajectory of (35) arrives in the boundary of the invariant set Ψ at $t = T_a$. According to the La Salle's Local Invariant Set Theorem [23], for $t \ge T_a$, $\overline{e}_{y,i}(t) \in \Psi$, namely $\overline{e}_{y,i}(t) \le \overline{e}_{y,i}(T_a)$. In the following, we will show $\overline{e}_{y,i}(T_a) \in (\varepsilon_{\delta,2}, \varepsilon_{\delta,1})$ by contradiction.

Suppose $\overline{e}_{y,i}(T_a) \ge \varepsilon_{\delta,1}$. Then from the adaptive law (23), it follows $\dot{\overline{\delta}}_i(T_a) = k_\delta > 0$. Hence at $t = T_a + \Delta t$ where Δt is the sampling time, $\overline{\delta}_i(T_a + \Delta t) > \overline{\delta}_i(T_a)$. Since $\dot{\overline{e}}_{y,i}(T_a) = 0$, $\overline{e}_{y,i}(T_a + \Delta t) = \overline{e}_{y,i}(T_a)$. Considering $h_1 \to 0$ exponentially, it follows from (35) that

$$\begin{aligned}&\dot{\overline{e}}_{y,i}(T_a + \Delta t)\\ =\ &\gamma\overline{e}_{y,i}(T_a + \Delta t) + \overline{\delta}_i(T_a + \Delta t) - \delta_i(T_a + \Delta t)\\ &-\mathrm{row}(A_3)_i h_1(T_a + \Delta t)\\ >\ &\gamma\overline{e}_{y,i}(T_a) + \overline{\delta}_i(T_a) - \delta_i(T_a) - \mathrm{row}(A_3)_i h_1(T_a)\\ =\ &\dot{\overline{e}}_{y,i}(T_a) = 0\end{aligned}$$

It implies $\overline{e}_{y,i}(T_a + 2\Delta t) > \overline{e}_{y,i}(T_a + \Delta t) = \overline{e}_{y,i}(T_a)$, which is in contradiction with the statement "for $t \ge T_a$, $\overline{e}_{y,i}(t) \le \overline{e}_{y,i}(T_a)$". Therefore, $\overline{e}_{y,i}(T_a) \ge \varepsilon_{\delta,1}$ does not hold and then $\overline{e}_{y,i}(T_a) < \varepsilon_{\delta,1}$. Similarly, we can get $\overline{e}_{y,i}(T_a) > \varepsilon_{\delta,2}$. Then $\overline{e}_{y,i}(T_a) \in (\varepsilon_{\delta,2}, \varepsilon_{\delta,1})$ is proved.

From (34) and the discussion below, it is known that $\overline{e}_{y,i}(t)$ will decrease from $\overline{e}_{y,i}(0)$ to $\overline{e}_{y,i}(T_a)$ and then converge to the invariant set Ψ, as shown in Fig. 3. From Fig. 3, it is clear that there exists a finite time T_s such that for $0 \le t \le T_s$, $\overline{e}_{y,i}(0) \le \overline{e}_{y,i}(t) \le \varepsilon_{\delta,1}$; for $t > T_s$, $\varepsilon_{\delta,2} < \overline{e}_{y,i}(t) < \varepsilon_{\delta,1}$. The

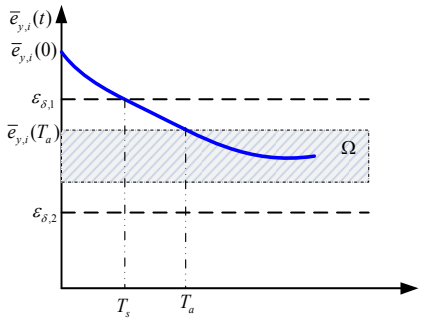

Fig. 3: The illustration of T_s.

similar conclusion on $\underline{e}_{y,i}(t)$ can be obtained. Therefore, Proposition 2 is proved. ■

Remark 8: By choosing γ and k_δ appropriately, it is possible to make $0 < T_s < T_F$, namely before the occurrence of the fault, $\varepsilon_{\delta,2}1_p \prec \overline{x}_2 - x_2 \prec \varepsilon_{\delta,1}1_p$ and $\varepsilon_{\delta,2}1_p \prec x_2 - \underline{x}_2 \prec \varepsilon_{\delta,1}1_p$ can be achieved.

In the following, an estimate of the disturbance d will be obtained.

Proposition 3: Denote

$$\begin{array}{l} \hat{d} = 0.5(\underline{d} + \overline{d}), \\ \overline{d} = (D_2^\dagger)^+\overline{\delta} - (D_2^\dagger)^-\underline{\delta}, \\ \underline{d} = (D_2^\dagger)^+\underline{\delta} - (D_2^\dagger)^-\overline{\delta} \end{array} \tag{39}$$

where $D_2^\dagger$ is the pseudo-inverse of D_2, then for $T_s < t < T_F$, the disturbance estimation error $\tilde{d} = d - \hat{d}$ is bounded by

$$\|\tilde{d}\| < \delta_d \triangleq 0.5\gamma(\varepsilon_{\delta,2} - \varepsilon_{\delta,1})\||D_2^\dagger|\| \tag{40}$$

where $|D_2^\dagger|$ is defined in Notation.

Proof: From Proposition 2 and Fig. 3, it follows that the trajectory of (35) enters the set $\{\varepsilon_{\delta,2} < \overline{e}_{y,i} < \varepsilon_{\delta,1}\}$ for $t > T_s$. Apply the Proposition 1 to (35), and it follows as $t \to \infty$, $\overline{e}_{y,i}(t) \to (\overline{\delta}_i - \delta_i - \mathrm{row}(A_3)_i h_1)/(-\gamma)$. Hence for $t > T_s$,

$$-\gamma\varepsilon_{\delta,2} < \overline{\delta}_i - \delta_i - \mathrm{row}(A_3)_i h_1 < -\gamma\varepsilon_{\delta,1} \tag{41}$$

Similarly, we can get for $t > T_s$

$$-\gamma\varepsilon_{\delta,2} < \delta_i - \underline{\delta}_i + \mathrm{row}(A_3)_i h_1 < -\gamma\varepsilon_{\delta,1} \tag{42}$$

Since $h_1 \to 0$ exponentially, it follows that as $t \to \infty$, (41) and (42) become

$$-\gamma\varepsilon_{\delta,2} < \overline{\delta}_i - \delta_i < -\gamma\varepsilon_{\delta,1}, -\gamma\varepsilon_{\delta,2} < \delta_i - \underline{\delta}_i < -\gamma\varepsilon_{\delta,1}$$

whose compact form for $i = 1, \cdots, p$ is

$$-\gamma\varepsilon_{\delta,2}1_p \prec \overline{\delta} - \delta \prec -\gamma\varepsilon_{\delta,1}1_p, -\gamma\varepsilon_{\delta,2}1_p \prec \delta - \underline{\delta} \prec -\gamma\varepsilon_{\delta,1}1_p \tag{43}$$

From Lemma 1 and (43), it follows that

$$\begin{array}{l} (D_2^\dagger)^+(-\gamma\varepsilon_{\delta,2}1_p) \prec (D_2^\dagger)^+(\overline{\delta} - \delta) \prec (D_2^\dagger)^+(-\gamma\varepsilon_{\delta,1}1_p) \\ (D_2^\dagger)^-(-\gamma\varepsilon_{\delta,2}1_p) \prec (D_2^\dagger)^-(\delta - \underline{\delta}) \prec (D_2^\dagger)^-(-\gamma\varepsilon_{\delta,1}1_p) \\ (D_2^\dagger)^+(-\gamma\varepsilon_{\delta,2}1_p) \prec (D_2^\dagger)^+(\underline{\delta} - \underline{\delta}) \prec (D_2^\dagger)^+(-\gamma\varepsilon_{\delta,1}1_p) \\ (D_2^\dagger)^-(-\gamma\varepsilon_{\delta,2}1_p) \prec (D_2^\dagger)^-(\overline{\delta} - \delta) \prec (D_2^\dagger)^-(-\gamma\varepsilon_{\delta,1}1_p) \end{array} \tag{44}$$

Considering $d = D_2^\dagger\delta = (D_2^\dagger)^+\delta - (D_2^\dagger)^-\delta$, it follows that

$$\begin{array}{rcl} \overline{d} - d & = & (D_2^\dagger)^+\overline{\delta} - (D_2^\dagger)^-\underline{\delta} - ((D_2^\dagger)^+\delta - (D_2^\dagger)^-\delta) \\ & = & (D_2^\dagger)^+(\overline{\delta} - \delta) + (D_2^\dagger)^-(\delta - \underline{\delta}) \end{array} \tag{45}$$

and

$$\begin{array}{rcl} d - \underline{d} & = & (D_2^\dagger)^+\delta - (D_2^\dagger)^-\delta - (D_2^\dagger)^+\underline{\delta} + (D_2^\dagger)^-\overline{\delta} \\ & = & (D_2^\dagger)^+(\delta - \underline{\delta}) + (D_2^\dagger)^-(\overline{\delta} - \delta) \end{array} \tag{46}$$

Combine (44), (45) with (46) to get

$$\begin{array}{l} |D_2^\dagger|(-\gamma\varepsilon_{\delta,2}1_p) \prec \overline{d} - d \prec |D_2^\dagger|(-\gamma\varepsilon_{\delta,1}1_p) \\ |D_2^\dagger|(-\gamma\varepsilon_{\delta,2}1_p) \prec d - \underline{d} \prec |D_2^\dagger|(-\gamma\varepsilon_{\delta,1}1_p) \end{array} \tag{47}$$

Since $\tilde{d} = 0.5(d - \underline{d}) - 0.5(\overline{d} - d)$ which when combined with (47), it follows that

$$|D_2^\dagger|0.5\gamma(\varepsilon_{\delta,1} - \varepsilon_{\delta,2})1_p \prec \tilde{d} \prec |D_2^\dagger|0.5\gamma(\varepsilon_{\delta,2} - \varepsilon_{\delta,1})1_p \tag{48}$$

and then (40) holds. ■

Remark 9: It is clear from Proposition 2 and Proposition 3 that when choosing $\varepsilon_{\delta,1}$ and $\varepsilon_{\delta,2}$ small enough, $\overline{x}_2$ and $\underline{x}_2$ are tight bounds of x_2; $\overline{d}$ and $\underline{d}$ are tight bounds of d. The conventional IO for (28) is given by [17]

$$\begin{array}{rcl} \dot{\overline{x}}_2 & = & \Gamma\overline{e}_y + A_3\hat{x}_1 + A_4 y + B_2 u + \overline{\delta}^c \\ \dot{\underline{x}}_2 & = & -\Gamma\underline{e}_y + A_3\hat{x}_1 + A_4 y + B_2 u + \underline{\delta}^c \end{array} \tag{49}$$

The conventional IO (49) has the similar structure as the proposed IO (22), whereas uses the conservative bounds of δ namely $\overline{\delta}^c$ and $\underline{\delta}^c$ from (29). Since $\overline{\delta}^c \succ \overline{\delta}$ and $\underline{\delta}^c \prec \underline{\delta}$ for $t > 0$, the bounds of states provided by the conventional IO (49) are loose. When using the conventional IO (49) for fault detection, a large fault missing alarm rate may be led.

B. Nominal controller

The nominal controller is designed as

$$u = K_n x_{es} \tag{50}$$

where

$$x_{es} = T^{-1}[x_{1,es}^T \; y^T]^T, x_{1,es} = \hat{x}_1 - \Lambda^{-1}\overline{D}_1\hat{d}, \tag{51}$$

$\hat{x}_1$ and $\hat{d}$ are from (21) and (39) respectively, K_n is a design parameter given in the following.

Theorem 1: By choosing K_n appropriately such that there exist a s.p.d. matrix P_n, $0 < \varepsilon_n < 1$ and $0 < \gamma_n \le \gamma_s$ making $\Omega_n < \mathbf{0}$, where

$$\Omega_n = \begin{bmatrix} (A + BK_n)^T P_n + P_n(A + BK_n) + (\varepsilon_n^2 + 1)I_n & P_n D \\ D^T P_n & -\gamma_n^2 I_q \end{bmatrix} \tag{52}$$

then the closed-loop system with (50) satisfies $\|x\| \le \gamma_s\|d\|$.

Proof: Substitute (50) into (2) to get the closed-loop system

$$\dot{x} = (A + BK_n)x - BK_n(x - x_{es}) + Dd \tag{53}$$

where when there are no sensor faults, $y = x_2$ and then

$$x - x_{es} = T^{-1}\left(\begin{bmatrix} x_1 \\ x_2 \end{bmatrix} - \begin{bmatrix} x_{1,es} \\ y \end{bmatrix}\right) = T^{-1}\begin{bmatrix} \tilde{x}_1 \\ \mathbf{0} \end{bmatrix} \tag{54}$$

where $\tilde{x}_1 = x_1 - x_{1,es}$. From (27),

$$x_1 = \hat{x}_1 + h_1 - \Lambda^{-1}\overline{D}_1 d \tag{55}$$

Subtract (51) from (55) to get

$$\tilde{x}_1 = h_1 - \Lambda^{-1}\bar{D}_1\tilde{d} \tag{56}$$

From $h_1 \to 0$ exponentially, it follows

$$\|\tilde{x}_1\| \le \|\Lambda^{-1}\bar{D}_1\|\delta_d \tag{57}$$

where δ_d is from (40).

Substitute (54) and (56) into (53), and it follows

$$\dot{x} = (A+BK_n)x - BK_{n1}\tilde{x}_1 + Dd \tag{58}$$

where $K_{n1} = K_n T^{-1}\begin{bmatrix} \mathbf{I}_{n-p} & \mathbf{0} \end{bmatrix}^T$. Take $V_n = x^T P_n x$ and its derivative is

$$\begin{aligned}\dot{V}_n &= x^T((A+BK_n)^T P_n + P_n(A+BK_n))x - 2x^T P_n BK_{n1}\tilde{x}_1 \\ &\quad +2x^T P_n Dd \\ &\le x^T((A+BK_n)^T P_n + P_n(A+BK_n))x + \varepsilon_n^2 x^T x \\ &\quad +2x^T P_n Dd + \tilde{x}_1^T K_{n1}^T B^T P_n P_n BK_{n1}\tilde{x}_1/\varepsilon_n^2\end{aligned}$$

where $0 < \varepsilon_n < 1$ is a constant. Define $W_n = \dot{V}_n + x^T x - \gamma_n^2 d^T d - \tilde{x}_1^T K_{n1}^T B^T P_n P_n BK_{n1}\tilde{x}_1/\varepsilon_n^2$, then $W_n \le \begin{bmatrix} x^T & d^T \end{bmatrix}\Omega_n \begin{bmatrix} x^T & d^T \end{bmatrix}^T$, where Ω_n is from (52). Since K_n is chosen to make $\Omega_n < \mathbf{0}$, then $W_n = \dot{V}_n + x^T x - \gamma_n^2 d^T d - \tilde{x}_1^T K_{n1}^T B^T P_n P_n BK_{n1}\tilde{x}_1/\varepsilon_n^2 < 0$. There are two cases:

Case 1 if $\dot{V}_n \ge 0$, then $x^T x - \gamma_n^2 d^T d - \tilde{x}_1^T K_{n1}^T B^T P_n P_n BK_{n1}\tilde{x}_1/\varepsilon_n^2 < 0$, namely $x^T x < \gamma_n^2 d^T d + \tilde{x}_1^T K_{n1}^T B^T P_n P_n BK_{n1}\tilde{x}_1/\varepsilon_n^2$;

Case 2 if $x^T x \ge \gamma_n^2 d^T d + \tilde{x}_1^T K_{n1}^T B^T P_n P_n BK_{n1}\tilde{x}_1/\varepsilon_n^2$, then $\dot{V}_n < 0$, which means $\|x(t)\| \le \|x(0)\|$ and $\Psi_n = \{x | x^T x < \gamma_n^2 d^T d + \tilde{x}_1^T K_{n1}^T B^T P_n P_n BK_{n1}\tilde{x}_1/\varepsilon_n^2\}$ is an invariant set. And when $t \to \infty$, $x(t) \to \Psi_n$.

In summary, for $t \ge 0$,

$$x^T x \le \max\{x(0)^T x(0), \gamma_n^2 d^T d + \tilde{x}_1^T K_{n1}^T B^T P_n P_n BK_{n1}\tilde{x}_1/\varepsilon_n^2\}$$

and when $t \to \infty$, from (57)

$$\begin{aligned}x^T x &< \gamma_n^2 d^T d + \tfrac{1}{\varepsilon_n^2}\tilde{x}_1^T K_{n1}^T B^T P_n P_n BK_{n1}\tilde{x}_1 \\ &< \gamma_n^2 d^T d + \tfrac{\lambda_{max}(K_{n1}^T B^T P_n P_n BK_{n1})}{\varepsilon_n^2}\|\tilde{x}_1\|^2 \\ &< \gamma_n^2 d^T d + \tfrac{\lambda_{max}(K_{n1}^T B^T P_n P_n BK_{n1})}{\varepsilon_n^2}\|\Lambda^{-1}\bar{D}_1\|^2\delta_d^2\end{aligned} \tag{59}$$

From (40) and Remark 9, by choosing $\varepsilon_{\delta,1}$ and $\varepsilon_{\delta,2}$ appropriately, it is possible that there exists a γ_m such that $\lambda_{max}(K_{n1}^T B^T P_n P_n BK_{n1})\|\Lambda^{-1}\bar{D}_1\|^2\delta_d^2/\varepsilon_n^2 \le \gamma_m^2 d^T d$ where $\gamma_n^2 + \gamma_m^2 \le \gamma_s^2$. Hence $\|x\| \le \gamma_s\|d\|$ is ensured. ■

Remark 10: Multiply the matrix $\mathrm{diag}\{P_n^{-1}, \mathbf{I}_q\}$ to both sides of Ω_n in (52), and define new variables $\hat{P}_n = P_n^{-1}$, $\hat{K}_n = K_n P_n^{-1}$, then it follows

$$\begin{bmatrix} \hat{P}_n A^T + \hat{K}_n^T B^T + A\hat{P}_n + B\hat{K}_n + (\varepsilon_n^2+1)\hat{P}_n^2 & D \\ D^T & -\gamma_n^2 I_q \end{bmatrix} < \mathbf{0}$$

Using the Schur complement [26], it further follows that

$$\begin{bmatrix} \hat{P}_n A^T + \hat{K}_n^T B^T + A\hat{P}_n + B\hat{K}_n & D & \sqrt{\varepsilon_n^2+1}\hat{P}_n \\ D^T & -\gamma_n^2 I_q & \mathbf{0} \\ \sqrt{\varepsilon_n^2+1}\hat{P}_n & \mathbf{0} & -\mathbf{I}_n \end{bmatrix} < \mathbf{0} \tag{60}$$

Thus, the inequality (52) is transformed into the LMI (60).

Remark 11: The LMI (60) only contains two variables $\hat{P}_n$ and $\hat{K}_n$, which when compared with the LMIs needed in [9, 10, 25], the computational cost is largely reduced. Moreover, the feasible condition for the LMI (60) is the controllability of the pair (A,B). However, when the sensors measuring the elevation/travel angles are faulty, the couple (A,C_r) is not detectable, and the LMIs needed in [9, 10, 25] are infeasible.

C. Fault Detection and Isolation

In this work, the proposed observer (22)-(23) acts not only as a state estimator for the nominal controller (50) but also as an FDI observer.

From (4), we have $x_2 = y - E_i f_{s,i}$ and (20) becomes

$$\dot{x}_1 = A_1 x_1 + A_2 y + F_{i1} f_{s,i} + B_1 u + \bar{D}_1 d \tag{61a}$$

$$\dot{x}_2 = A_3\tilde{x}_1 + A_3\hat{x}_1 + A_4 y + F_{i2} f_{s,i} + B_2 u + \bar{D}_2 d \tag{61b}$$

$$\dot{y} = A_3\tilde{x}_1 + A_3\hat{x}_1 + A_4 y + F_{i2} f_{s,i} + B_2 u + \bar{D}_2 d + E_i\dot{f}_{s,i} \tag{61c}$$

where $F_{i1} = -A_2 E_i$, $F_{i2} = -A_4 E_i$.

Subtract (21) from (61a) and (22) from (61c) to get

$$\dot{\tilde{x}}_1 = A_1\tilde{x}_1 + \bar{D}_1 d + F_{i1} f_{s,i} \tag{62a}$$

$$\begin{aligned}\dot{\bar{e}}_y &= \Gamma\bar{e}_y + \bar{\delta} - \Delta - E_i\dot{f}_{s,i} \\ \dot{\underline{e}}_y &= \Gamma\underline{e}_y + \Delta - \underline{\delta} + E_i\dot{f}_{s,i}\end{aligned} \tag{62b}$$

where $\Delta = A_3\tilde{x}_1 + \bar{D}_2 d + F_{i2} f_{s,i}$. From the structure of E_i, the component form of (62b) can be divided into two cases

- Case 1: for $j = 1, \cdots, p$ and $j \ne i$,

$$\dot{\bar{e}}_{y,j} = \gamma\bar{e}_{y,j} + \bar{\delta}_j - \Delta_j, \dot{\underline{e}}_{y,j} = \gamma\underline{e}_{y,j} + \Delta_j - \underline{\delta}_j \tag{63}$$

  From Proposition 2 and Remark 8, it is known that for $t \in (T_s, T_F)$, $\varepsilon_{\delta,2} < \bar{e}_{y,j} < \varepsilon_{\delta,1}$ and $\dot{\bar{\delta}}_j = 0$. For $t \ge T_F$, two scenarios should be considered. In the first scenario, $\dot{\bar{e}}_{y,j}(T_F) > 0$, as shown in Fig. 4, $\bar{e}_{y,j}(t)$ will increase; if $\bar{e}_{y,j}(t) \ge \varepsilon_{\delta,1}$, the adaptive law (23) becomes $\dot{\bar{\delta}}_j < 0$ which implies that $\bar{\delta}_j$ decreases and so does $\dot{\bar{e}}_{y,j}$ until $\varepsilon_{\delta,2} < \bar{e}_{y,j} < \varepsilon_{\delta,1}$ again. Hence for this scenario, $y_j \in [\underline{y}_j, \bar{y}_j]$ holds. In the other scenario, $\dot{\bar{e}}_{y,j}(T_F) < 0$, as shown in Fig. 5, $\bar{e}_{y,j}(t)$ will decrease; if $\bar{e}_{y,j}(t) \le \varepsilon_{\delta,2}$, the adaptive law (23) becomes $\dot{\bar{\delta}}_j > 0$ which implies that $\bar{\delta}_j$ increases and so does $\dot{\bar{e}}_{y,j}$ until $\varepsilon_{\delta,2} < \bar{e}_{y,j} < \varepsilon_{\delta,1}$ again. Note that k_δ should be chosen appropriately such that

$$\text{when } \dot{\bar{e}}_{y,j}(T_c) = 0, \bar{e}_{y,j}(T_c) \ge 0 \tag{64}$$

  Hence for this scenario, $y_j \in [\underline{y}_j, \bar{y}_j]$ still holds. In summary, for Case 1, $y_j \in [\underline{y}_j, \bar{y}_j]$ for $t \ge 0$.

- Case 2: for $j = i$, $\dot{\bar{e}}_{y,i} = \gamma\bar{e}_{y,i} + \bar{\delta}_i - \Delta_i - \dot{f}_{s,i}$ and $\dot{\underline{e}}_{y,i} = \gamma\underline{e}_{y,i} + \Delta_i - \underline{\delta}_i + \dot{f}_{s,i}$. It is clear that the dynamics of $\dot{\bar{e}}_{y,i}$ and $\dot{\underline{e}}_{y,i}$ contain $\dot{f}_{s,i}$. From Remark 1, $\dot{f}_{s,i}(T_F) = \infty$ which may make $\bar{e}_{y,i}$ change abruptly and then $y_i \notin [\underline{y}_i, \bar{y}_i]$. In this case, although $\bar{\delta}_i$ and $\underline{\delta}_i$ change according to (23), it still needs a period of time such that $\bar{\delta}_i > \Delta_i + \dot{f}_{s,i}$ and $\underline{\delta}_i < \Delta_i + \dot{f}_{s,i}$ to ensure $y_i \in [\underline{y}_i, \bar{y}_i]$.

In summary, the FDI mechanism is

- if for $t \ge 0$, $y_i \in [\underline{y}_i, \bar{y}_i]$ for all $i = 1, \cdots, p$, then all sensors are healthy;

- if there exists a period of time $t \in [T^d, T^s]$ where $T^s > T^d \geq T_F$ such that $y_i \notin [\underline{y}_i, \overline{y}_i]$ and $y_j \in [\underline{y}_j, \overline{y}_j]$ for all $j = 1, \cdots, p$ and $j \neq i$, then the ith sensor is faulty, and the fault detection and isolation time is T^d.

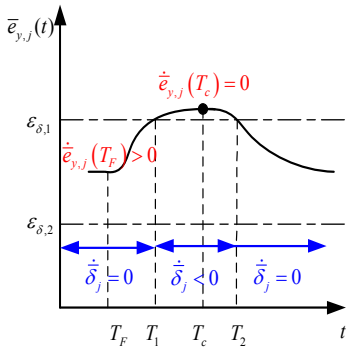

Fig. 4: The illustration of Scenario 1 in Case 1.

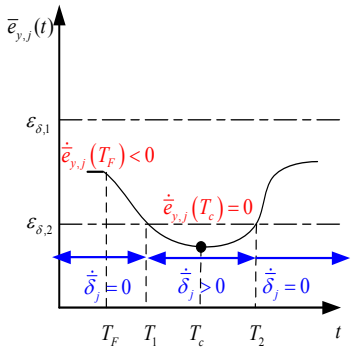

Fig. 5: The illustration of Scenario 2 in Case 1.

Remark 12: Different from the existing FDI schemes which require a set of observers [18], this work utilizes only one adaptive IO (22) to acquire the occurrence and location of fault simultaneously, not only reducing the computation cost but also shortening the fault diagnosis time.

Remark 13: For $t \geq T_F$, from (63) and the discussion in Case 1, it is known that when $\varepsilon_{\delta,2} < \bar{e}_{y,j} < \varepsilon_{\delta,1}$ holds again, $\overline{\delta}_j$ and $\underline{\delta}_j$ are no longer the tight bounds of δ_j but Δ_j. Hence the estimate of d in (39) for should be changed into

$$\begin{aligned} &\hat{d} = 0.5(\underline{d} + \overline{d}), \\ &\overline{d} = \begin{cases} (D_2^\dagger)^+ \overline{\delta}(t) - (D_2^\dagger)^- \underline{\delta}(t), & 0 \leq t < T^d \\ (D_2^\ddagger)^+ \overline{\delta}(T_s) - (D_2^\dagger)^- \underline{\delta}(T_s), & t \geq T^d \end{cases}, \\ &\underline{d} = \begin{cases} (D_2^\dagger)^+ \underline{\delta}(T_s) - (D_2^\dagger)^- \overline{\delta}(T_s), & 0 \leq t < T^d \\ (D_2^\ddagger)^+ \underline{\delta}(T_s) - (D_2^\ddagger)^- \overline{\delta}(T_s), & t \geq T^d \end{cases} \end{aligned} \tag{65}$$

IV. Fault Tolerant Control

From the proposed FDI mechanism, we can determine the location of sensor fault. In this section, fault tolerant control (FTC) scheme based on two different fault estimation (FE) units is constructed to ensure the acceptable system performance (9).

Introduce the following auxiliary dynamics from (8)

$$\dot{x}_f = A_f x_f + y_f = A_f x_f + \text{row}(C)_i x + f_{s,i} \tag{66}$$

Combine (2) with (66) and define $y_{new} = [y_r^T \ x_f^T]^T$ to get the following augmented system

$$\dot{\xi} = A_a \xi + B_a u + F_a f_{s,i} + D_a d, y_{new} = C_a \xi \tag{67}$$

where $\xi = \begin{bmatrix} x \\ x_f \end{bmatrix}$, $A_a = \begin{bmatrix} A & \mathbf{0} \\ \text{row}(C)_i & A_f \end{bmatrix}$, $B_a = \begin{bmatrix} B \\ \mathbf{0} \end{bmatrix}$, $F_a = \begin{bmatrix} \mathbf{0} \\ 1 \end{bmatrix}$, $D_a = \begin{bmatrix} D \\ \mathbf{0} \end{bmatrix}$, $C_a = \begin{bmatrix} C_r & \mathbf{0} \\ \mathbf{0} & 1 \end{bmatrix}$.

Remark 14: For the augmented system (67), it is clear that $\text{rank}(C_a F_a) = \text{rank}(F_a)$ and the pair (A_a, C_a) is observable; only when the pair (A, C_r) is detectable, the triple (A_a, F_a, C_a) is minimum phase.

From Remark 14, the judgement condition is proposed:

Condition 1: The couple (A, C_r) is detectable.

According to the condition 1, the FE schemes will be designed respectively for the following cases: Case 1 (A, C_r) is detectable, Case 2 (A, C_r) is not detectable.

A. Fault estimation for Case 1

Since $\text{rank}(C_a F_a) = \text{rank}(F_a)$ and (A_a, C_a) is observable, the state transformation similar to those in Section III-A will be introduced for the system (67), making

$$\begin{aligned} &\xi \to \begin{bmatrix} \xi_1 \\ \xi_2 \end{bmatrix}, A_a \to \begin{bmatrix} \mathscr{A}_1 & \mathscr{A}_2 \\ \mathscr{A}_3 & \mathscr{A}_4 \end{bmatrix}, B_a \to \begin{bmatrix} \mathscr{B}_1 \\ \mathscr{B}_2 \end{bmatrix}, \\ &F_a \to \begin{bmatrix} \mathbf{0} \\ \mathscr{F}_2 \end{bmatrix}, D_a \to \begin{bmatrix} \mathscr{D}_1 \\ \mathscr{D}_2 \end{bmatrix}, C_a \to [\mathbf{0} \ \mathbf{I}_p], \end{aligned} \tag{68}$$

where $\mathscr{F}_2$ is full of column rank, $\mathscr{F}_2 f_{s,i} \triangleq f$, $\mathscr{A}_1 \approx \Lambda$ with Λ from (18).

The observers with the similar structure as (21), (22) and (23) are proposed

$$\dot{\hat{\xi}}_1 = \mathscr{A}_1 \hat{\xi}_1 + \mathscr{A}_2 y_{new} + \mathscr{B}_1 u + \mathscr{D}_1 \hat{d} \tag{69a}$$

$$\begin{aligned} \dot{\overline{\xi}}_2 &= \Gamma_a \overline{e}_Y + \mathscr{A}_3 \hat{\xi}_1 + \mathscr{A}_4 y_{new} + \mathscr{B}_2 u + \overline{f} + \mathscr{D}_2 \hat{d} \\ \dot{\underline{\xi}}_2 &= -\Gamma_a \underline{e}_Y + \mathscr{A}_3 \hat{\xi}_1 + \mathscr{A}_4 y_{new} + \mathscr{B}_2 u + \underline{f} + \mathscr{D}_2 \hat{d} \end{aligned} \tag{69b}$$

where $\hat{d}$ is from (65). $\Gamma_a = \text{diag}\{\gamma_a\}$ and $\gamma_a < 0$ is a user-defined scalar. $\overline{e}_Y = \overline{y}_{new} - y_{new}$, $\underline{e}_Y = y_{new} - \underline{y}_{new}$, $\underline{y}_{new} = \underline{\xi}_2$, $\overline{y}_{new} = \overline{\xi}_2$. And $\overline{f} = [\overline{f}_1, \cdots, \overline{f}_p]$, $\underline{f} = [\underline{f}_1, \cdots, \underline{f}_p]$, $\underline{f}_i$, $\overline{f}_i, i = 1, \cdots, p$ are determined by the following adaptive laws:

$$\begin{aligned} \dot{\overline{f}}_i &= -k_f(\text{sgn}(\overline{e}_{Y,i} - \varepsilon_{f,1}) + \text{sgn}(\overline{e}_{Y,i} - \varepsilon_{f,2})) \\ \dot{\underline{f}}_i &= k_f(\text{sgn}(\underline{e}_{Y,i} - \varepsilon_{f,1}) + \text{sgn}(\underline{e}_{Y,i} - \varepsilon_{f,2})) \end{aligned} \tag{70}$$

where $\overline{e}_{Y,i}$ and $\underline{e}_{Y,i}$ are the i-th component of $\overline{e}_Y$ and $\underline{e}_Y$ respectively, and $\varepsilon_{f,1} > \varepsilon_{f,2} > 0$ are user-defined constants which determine the width of $\overline{e}_{Y,i}$ and $\underline{e}_{Y,i}$, and $k_f > 0$ is a user-defined constant which determines the changing rates of $\overline{f}_i$ and $\underline{f}_i$. The initial value $\hat{\xi}_1(0)$ is arbitrary. Choose $\overline{\xi}_2(0)$ and $\underline{\xi}_2(0)$ arbitrarily. $\underline{f}_i(0) = 0$ and $\overline{f}_i(0) = 0$ are the initial values of $\underline{f}_i$ and $\overline{f}_i$ respectively.

Theorem 2: When Condition 1 holds, the FE scheme (69)-(70) can achieve $\hat{f}_{s,i} \approx f_{s,i}$ with $\hat{f}_{s,i} = 0.5\mathscr{F}_2^\dagger(\underline{f} + \overline{f})$, $\mathscr{F}_2^\dagger$ is the pseudo-inverse of $\mathscr{F}_2$. If $\varepsilon_{f,1}$, $\varepsilon_{f,2}$ and $\varepsilon_{\delta,1}$, $\varepsilon_{\delta,2}$ are chosen small enough, then the fault estimation error is small.

Proof: Define $\tilde{\xi}_1 = \xi_1 - \hat{\xi}_1$, then subtract (69a) from (68) to get

$$\dot{\tilde{\xi}}_1 = \mathscr{A}_1 \tilde{\xi}_1 + \mathscr{D}_1 \tilde{d} \approx \Lambda \tilde{\xi}_1 + \mathscr{D}_1 \tilde{d} \tag{71}$$

From Proposition 1 (set $P_e = \mathbf{I}$), we have

$$\|\tilde{\xi}_1\| \leq \frac{\|\mathscr{D}_1\|\|\tilde{d}\|}{-\lambda} \tag{72}$$

By subtracting (69b) from (68), the dynamics of $\overline{e}_Y$ and $\underline{e}_Y$ are obtained as

$$\begin{aligned} \dot{\overline{e}}_Y &= \Gamma_a \overline{e}_Y + \overline{f} - f - \mathscr{D}_2\tilde{d} - \mathscr{A}_3\tilde{\xi}_1 \\ \dot{\underline{e}}_Y &= \Gamma_a \underline{e}_Y + f - \underline{f} + \mathscr{D}_2\tilde{d} + \mathscr{A}_3\tilde{\xi}_1 \end{aligned} \tag{73}$$

Similar to the proof of Proposition 3, it follows that

$$\begin{aligned} -\gamma_a\varepsilon_{f,2}\mathbf{1}_p + \mathscr{D}_2\tilde{d} + \mathscr{A}_3\tilde{\xi}_1 < \overline{f} - f < -\gamma_a\varepsilon_{f,1}\mathbf{1}_p + \mathscr{D}_2\tilde{d} + \mathscr{A}_3\tilde{\xi}_1 \\ -\gamma_a\varepsilon_{f,2}\mathbf{1}_p - \mathscr{D}_2\tilde{d} - \mathscr{A}_3\tilde{\xi}_1 < f - \underline{f} < -\gamma_a\varepsilon_{f,1}\mathbf{1}_p - \mathscr{D}_2\tilde{d} - \mathscr{A}_3\tilde{\xi}_1 \end{aligned}$$

which imply

$$\begin{aligned} &\gamma_a(\varepsilon_{f,1} - \varepsilon_{f,2})\mathbf{1}_p - 2\mathscr{D}_2\tilde{d} - 2\mathscr{A}_3\tilde{\xi}_1 < f - \underline{f} + f - \overline{f} \\ &< \gamma_a(\varepsilon_{f,2} - \varepsilon_{f,1})\mathbf{1}_p - 2\mathscr{D}_2\tilde{d} - 2\mathscr{A}_3\tilde{\xi}_1 \end{aligned} \tag{74}$$

Combine (74) with (40) and (72) to get

$$\begin{aligned} & \|f - \underline{f} + f - \overline{f}\| \\ \leq\ & \gamma_a\sqrt{p}(\varepsilon_{f,2} - \varepsilon_{f,1}) + 2\|\mathscr{D}_2\|\|\tilde{d}\| + 2\|\mathscr{A}_3\|\|\tilde{\xi}_1\| \\ \leq\ & \gamma_a\sqrt{p}(\varepsilon_{f,2} - \varepsilon_{f,1}) + 2\left(\|\mathscr{D}_2\| + \frac{\|\mathscr{A}_3\|\|\mathscr{D}_1\|}{-\lambda}\right)\|\tilde{d}\| \\ \leq\ & \gamma_a\sqrt{p}(\varepsilon_{f,2} - \varepsilon_{f,1}) + 2\left(\|\mathscr{D}_2\| + \frac{\|\mathscr{A}_3\|\|\mathscr{D}_1\|}{-\lambda}\right)\delta_d \end{aligned} \tag{75}$$

Define $\tilde{f}_{s,i} = f_{s,i} - \hat{f}_{s,i}$, then from (75)

$$\begin{aligned} |\tilde{f}_{s,i}| &= |f_{s,i} - \hat{f}_{s,i}| \\ &= |0.5\mathscr{F}_2^\dagger(f + f) - 0.5\mathscr{F}_2^\dagger(\underline{f} + \overline{f})| \\ &= |0.5\mathscr{F}_2^\dagger(f - \underline{f} + f - \overline{f})| \\ &\leq 0.5\|\mathscr{F}_2^\dagger\|\|f - \underline{f} + f - \overline{f}\| \\ &\leq 0.5\|\mathscr{F}_2^\dagger\|\gamma_a\sqrt{p}(\varepsilon_{f,2} - \varepsilon_{f,1}) \\ &\quad + \|\mathscr{F}_2^\dagger\|\left(\|\mathscr{D}_2\| + \frac{\|\mathscr{A}_3\|\|\mathscr{D}_1\|}{-\lambda}\right)\delta_d \triangleq \delta_f^1 \end{aligned} \tag{76}$$

From Remark 9, when $\varepsilon_{f,1}$, $\varepsilon_{f,2}$ and $\varepsilon_{\delta,2}$, $\varepsilon_{\delta,1}$ are chosen small enough, $\hat{f}_{s,i}$ is a good estimation of $f_{s,i}$. ■

B. Fault estimation for Case 2

When (A, C_r) is not detectable, the triple (A_a, F_a, C_a) is non-minimum phase. Hence the FE scheme (69)-(70) cannot be adopted.

The dynamics of $\tilde{x}_1$ when the ith sensor is faulty can be obtained by subtracting (21) from (61a) as

$$\dot{\tilde{x}}_1 = A_1\tilde{x}_1 + F_{i1}f_{s,i} + \bar{D}_1 d \tag{77}$$

which is solved to get

$$\tilde{x}_1(t) = h_1 - \Lambda^{-1}\bar{D}_1 d + \int_0^t e^{\Lambda(t-\tau)}F_{i1}f_{s,i}(\tau)d\tau \tag{78}$$

Define x_{2r}, A_{3r}, A_{4r}, B_{2r}, C_r and $\bar{D}_{2r}$ according to Notations, then from (61b) and (78) we have

$$\begin{aligned} \dot{x}_{2r} &= A_{4r}y + B_{2r}u + A_{3r}h_1 + A_{3r}\int_0^t e^{\Lambda(t-\tau)}F_{i1}f_{s,i}(\tau)d\tau \\ &\quad + A_{3r}\hat{x}_1 + \underbrace{(-A_{4r}E_i)}_{F_{2r}}f_{s,i} + \underbrace{(\bar{D}_{2r} - A_{3r}\Lambda^{-1}\bar{D}_1)}_{D_{2r}}d, \\ y_r &= x_{2r} = C_r x \end{aligned} \tag{79}$$

For Case 2, the sensor fault $f_{s,i}$ is estimated as

$$\begin{aligned} \dot{\hat{f}}_{s,i} + c_{s,j}\hat{f}_{s,i} &= \frac{1}{\mathrm{row}(F_{2r})_j}\left(-\lambda(\nu_{r,j})_{eq} + (\dot{\nu_{r,j}})_{eq}\right) \\ &\quad + \frac{\lambda\,\mathrm{row}(D_{2r})_j}{\mathrm{row}(F_{2r})_j}\hat{d} \end{aligned} \tag{80}$$

where λ and $\hat{d}$ are from (18) and (65) respectively.

$$c_{s,j} = -\lambda + \frac{\mathrm{row}(A_{3r})_j F_{i1}}{\mathrm{row}(F_{2r})_j} \tag{81}$$

$(\dot{\nu_{r,j}})_{eq}$ is the derivative of $(\nu_{r,j})_{eq}$ with respect to time, $(\nu_{r,j})_{eq}$ is the equivalent output injection of $\nu_{r,j}$ [24]. $\nu_{r,j} = \rho_j\mathrm{sgn}(\tilde{x}_{2r,j})$, $\rho_j > 0$ is a design constant, $\tilde{x}_{2r,j}$ is the jth component of $\tilde{x}_{2r}$. $\tilde{x}_{2r} = x_{2r} - \hat{x}_{2r}$ with $\hat{x}_{2r}$ from the following sliding mode observer (SMO)

$$\dot{\hat{x}}_{2r} = -\Gamma_m\tilde{x}_{2r} + A_{3r}\hat{x}_1 + A_{4r}y + B_{2r}u + \nu_r \tag{82}$$

where $\Gamma_m = \mathrm{diag}\{\gamma_m\}$ with $\gamma_m < 0$. $\nu_r = [\nu_{r,1}, \cdots, \nu_{r,p-1}]^T$.

Theorem 3: When Condition 1 does not hold, if $c_{s,j} > 0$ for $j = 1, \mathrm{or}, \cdots, \mathrm{or}, p-1$ and $\varepsilon_{\delta,1}$, $\varepsilon_{\delta,2}$ are chosen small enough, then the FE scheme (82)-(80) ensures $\hat{f}_{s,i} \approx f_{s,i}$.

Proof: Subtract (82) from (79) to get

$$\dot{\tilde{x}}_{2r} = \Gamma_m\tilde{x}_{2r} + \Delta_{2r} - \nu_r \tag{83}$$

where $\Delta_{2r} = A_{3r}h_1 + A_{3r}\int_0^t e^{\Lambda(t-\tau)}F_{i1}f_{s,i}(\tau)d\tau + F_{2r}f_{s,i} + D_{2r}d$. From the structure of Γ_m, the component form of (83) is given by

$$\dot{\tilde{x}}_{2r,j} = \gamma_m\tilde{x}_{2r,j} + \Delta_{2r,j} - \nu_{r,j}$$

By choosing ρ_j appropriately, $\tilde{x}_{2r,j} \to 0$ and $\dot{\tilde{x}}_{2r,j} \to 0$ in finite time. When $\tilde{x}_{2r,j} = 0$ and $\dot{\tilde{x}}_{2r,j} = 0$, from the equivalent output injection technique [24], it follows that for $j = 1, \cdots, p-1$, $\Delta_{2r,j} = (\nu_{r,j})_{eq}$, which can be further written as

$$\begin{aligned} &\mathrm{row}(A_{3r})_j h_1 + \mathrm{row}(A_{3r})_j\int_0^t e^{\lambda(t-\tau)}F_{i1}f_{s,i}(\tau)d\tau + \mathrm{row}(F_{2r})_j f_{s,i} \\ &+\mathrm{row}(D_{2r})_j d = (\nu_{r,j})_{eq} \end{aligned} \tag{84}$$

which is a Volterra integral equation (VIE) about $f_{s,i}$. Multiply $e^{-\lambda t}$ to both sides of (84) to get

$$\begin{aligned} &e^{-\lambda t}\mathrm{row}(A_{3r})_j h_1 + \mathrm{row}(A_{3r})_j\int_0^t e^{-\lambda\tau}F_{i1}f_{s,i}(\tau)d\tau \\ &+e^{-\lambda t}\mathrm{row}(F_{2r})_j f_{s,i} + e^{-\lambda t}\mathrm{row}(D_{2r})_j d = e^{-\lambda t}(\nu_{r,j})_{eq} \end{aligned} \tag{85}$$

which is differentiated once and rearranged to get

$$\begin{aligned} &\mathrm{row}(F_{2r})_j\dot{f}_{s,i} + (\mathrm{row}(A_{3r})_j F_{i1} - \lambda\,\mathrm{row}(F_{2r})_j)f_{s,i} + \\ &\mathrm{row}(A_{3r})_j\dot{h}_1 - \lambda\,\mathrm{row}(A_{3r})_j h_1 - \lambda\,\mathrm{row}(D_{2r})_j d \\ &= (\dot{\nu_{r,j}})_{eq} - \lambda(\nu_{r,j})_{eq} \end{aligned} \tag{86}$$

From (86), it further follows that for $j = 1, \cdots, p-1$

$$\begin{aligned} &\dot{f}_{s,i} + c_{s,j}f_{s,i} = \frac{1}{\mathrm{row}(F_{2r})_j}\left(-\lambda(\nu_{r,j})_{eq} + (\dot{\nu_{r,j}})_{eq}\right) \\ &+\frac{1}{\mathrm{row}(F_{2r})_j}(-\mathrm{row}(A_{3r})_j\dot{h}_1 + \lambda\,\mathrm{row}(A_{3r})_j h_1 + \lambda\,\mathrm{row}(D_{2r})_j d) \end{aligned} \tag{87}$$

Define $\tilde{f}_{s,i} = f_{s,i} - \hat{f}_{s,i}$ and subtract (80) from (87) to get

$$\begin{aligned} &\dot{\tilde{f}}_{s,i} = -c_{s,j}\tilde{f}_{s,i} + \frac{1}{\mathrm{row}(F_{2r})_j}(-\mathrm{row}(A_{3r})_j\dot{h}_1 + \lambda\,\mathrm{row}(A_{3r})_j h_1 \\ &+\lambda\,\mathrm{row}(D_{2r})_j\tilde{d}) \end{aligned} \tag{88}$$

Since $h_1 \to 0$ and $\dot{h}_1 \to 0$ exponentially, when $t \to \infty$,

$$\dot{\tilde{f}}_{s,i} = -c_{s,j}\tilde{f}_{s,i} + \frac{\lambda\,\mathrm{row}(D_{2r})_j}{\mathrm{row}(F_{2r})_j}\tilde{d} \tag{89}$$

If $c_{s,j} > 0$ for $j = 1, \text{or}, \cdots, \text{or}, p-1$, then according to Proposition 1 and (40),

$$|\tilde{f}_{s,i}| \leq \left| \frac{\lambda \text{row}(D_{2r})_j}{c_{s,j}\text{row}(F_{2r})_j} \right| \|\tilde{d}\| \leq \left| \frac{\lambda \text{row}(D_{2r})_j}{c_{s,j}\text{row}(F_{2r})_j} \right| \delta_d \triangleq \delta_f^2 \quad (90)$$

From Remark 9, when $\varepsilon_{\delta,1}$ and $\varepsilon_{\delta,2}$ are chosen small enough, $\hat{f}_{s,i}$ is a good estimate of $f_{s,i}$. ■

Remark 15: From the proof of Theorem 3, it is known that $c_{s,j} > 0$ is important for the convergence of the fault estimation error. Since (A,C) is observable, from the discussion in Section III-A, the eigenvalues $\lambda_1 \approx \cdots \approx \lambda_{n-p} \approx \lambda$ can be arbitrarily assigned. Hence there must be an appropriate λ such that $c_{s,j} > 0$ in (81).

Remark 16: Summarize Theorem 2 with Theorem 3, and it follows that $|\tilde{f}_{s,i}| \leq \delta_f = \max\{\delta_f^1, \delta_f^2\}$. If $\varepsilon_{f,1}$, $\varepsilon_{f,2}$ and $\varepsilon_{\delta,1}$, $\varepsilon_{\delta,2}$ are chosen small enough, then the fault estimation error is small.

Remark 17: When the sensors measuring elevation and travel angles are faulty, the detectability with respect to the remaining healthy outputs is lost, resulting in established FE-based sensor FTC methods [9, 10] are not applicable. To circumvent this problem, a novel FE scheme based on sliding mode equivalent output injection and VIE is proposed to obtain the fault estimate.

C. Fault tolerant controller

From Theorem 2 and Theorem 3, the sensor fault estimate $\hat{f}_{s,i}$ is obtained and then used to develop the fault tolerant controller as

$$u = K_n x_f \quad (91)$$

where

$$\begin{array}{l} x_f = T^{-1}[x_{1,f}^T \ \hat{y}]^T, \hat{y} = y - \hat{f}_s, \hat{f}_s = E_i \hat{f}_{s,i}, \\ x_{1,f} = \hat{x}_1 - \Lambda^{-1}\bar{D}_1 \hat{d} + \int_0^t e^{\Lambda(t-\tau)} F_{i1} \hat{f}_{s,i}(\tau) d\tau \end{array} \quad (92)$$

K_n is from (52), $\hat{x}_1$ and $\hat{d}$ are from (21) and (65) respectively, $\hat{f}_{s,i}$ is from Theorem 2 when Condition 1 holds, otherwise, from Theorem 3.

Theorem 4: The proposed fault tolerant controller (91) can ensure the acceptable performance (9) of the faulty system.

Proof: Denote $\tilde{x}_{1,f} = x_1 - x_{1,f}$, and then subtract (92) from (78) to get

$$\tilde{x}_{1,f} = h_1 - \Lambda^{-1}\bar{D}_1 \tilde{d} + \int_0^t e^{\Lambda(t-\tau)} F_{i1} \tilde{f}_{s,i}(\tau) d\tau \quad (93)$$

and then from (40)

$$\begin{array}{rcl} \|\tilde{x}_{1,f}\| & \leq & \|h_1\| + \|\Lambda^{-1}\bar{D}_1\| \|\tilde{d}\| + \int_0^t e^{\lambda(t-\tau)} \|F_{i1}\| \|\tilde{f}_{s,i}(\tau)\| d\tau \\ & \leq & \|h_1\| + \|\Lambda^{-1}\bar{D}_1\| \delta_d + \frac{\|F_{i1}\|\delta_f}{-\lambda}(1 - e^{\lambda t}) \end{array} \quad (94)$$

Since $h_1 \to 0$ and $e^{\lambda t} \to 0$ as $t \to \infty$, (94) becomes

$$\|\tilde{x}_{1,f}\| \leq \|\Lambda^{-1}\bar{D}_1\| \delta_d + \frac{\|F_{i1}\|\delta_f}{-\lambda} \quad (95)$$

Substitute (91) into (2) to get the closed-loop system

$$\dot{x} = (A + BK_n)x - BK_n(x - x_f) + Dd \quad (96)$$

where

$$x - x_f = T^{-1}\left(\begin{bmatrix} x_1 \\ x_2 \end{bmatrix} - \begin{bmatrix} x_{1,f} \\ \hat{y} \end{bmatrix} \right) = T^{-1} \begin{bmatrix} \tilde{x}_{1,f} \\ -E_i \tilde{f}_{s,i} \end{bmatrix} \quad (97)$$

Similar to the proof of Theorem 1, it follows that when $t \to \infty$,

$$\begin{array}{rcl} x^T x & < & \gamma_n^2 d^T d + (x - x_f)^T K_n^T B^T P_n P_n B K_n (x - x_f)/\varepsilon_n^2 \\ & < & \gamma_n^2 d^T d + \lambda_{max}(K_n^T B^T P_n P_n B K_n)\|x - x_f\|^2/\varepsilon_n^2 \\ & < & \gamma_n^2 d^T d + \lambda_{max}(K_n^T B^T P_n P_n B K_n)\lambda_{max}(T^{-T}T^{-1}) \\ & & (\|\tilde{x}_{1,f}\|^2 + \|\tilde{f}_{s,i}\|^2)/\varepsilon_n^2 \end{array}$$

If $\varepsilon_{f,1}$, $\varepsilon_{f,2}$ and $\varepsilon_{\delta,1}$, $\varepsilon_{\delta,2}$ are chosen small enough, it is possible that there exists a γ_m such that $\lambda_{max}(K_n^T B^T P_n P_n B K_n)\lambda_{max}(T^{-T}T^{-1})(\|\tilde{x}_{1,f}\|^2 + \|\tilde{f}_{s,i}\|^2)/\varepsilon_n^2 \leq \gamma_m^2 d^T d$ where $\gamma_n^2 + \gamma_m^2 \leq \gamma_s^2$. Hence when $t \to \infty$, $\|x\| \leq \gamma_s \|d\|$ holds. ■

Remark 18: The proposed FTC scheme includes one Condition 1 and two FE units (Theorem 2 and Theorem 3), and moreover only uses the attitude angles. To the best knowledge of authors, most works on FTC of 3-DOF helicopter assumed that both attitude and velocity are available [3, 5].

V. Simulations and Experiments

Here, we verify the proposed scheme on the 3-DOF laboratory helicopter by both simulations and experiments. The helicopter setup is manufactured by Quanser Consulting Inc. [19]. We consider the following two cases: Case 1, the 2nd sensor has a fault $f_{s,2}$; Case 2, the 3rd sensor has a fault $f_{s,3}$. The sensor fault $f_{s,i}, i = 2,3$ has the structure of (5) with $\alpha = 1$, $T_F = 20$ sec, $f_{s,i}^* = 0.05$.

A. Results of fault diagnosis

Fault diagnosis results for Case 1 and Case 2 with the proposed scheme in Section III-C are shown in Fig. 6 and Fig. 7, respectively. From Fig. 6, it can be seen that y_1 and y_3 are always within their upper and lower bounds (moreover, the bounds are very tight), and however, y_2 is beyond its bounds at $t \in [20, 20.19]$sec. Hence it is concluded that the sensor measuring y_2 has a fault at about 20sec for Case 1. From Fig. 7, it can be seen that y_1 and y_2 are always within their upper and lower bounds, and however, y_3 is beyond its bounds at $t \in [20, 20.18]$sec. Hence, it is concluded that the sensor measuring y_3 has a fault about 20sec for Case 2.

To better show the fault diagnosis performances of the proposed IO (22), a comparison with the conventional IO (49) is conducted here. The outputs (y) and their bounds ($\bar{y} = \bar{x}_2$ and $\underline{y} = \underline{x}_2$) from the conventional IO (49) are shown in Fig. 8 and Fig. 9 for Case 1 and Case 2 respectively. It is clear that for two cases the outputs are always within their bounds, and moreover, the distances between the outputs and their bounds are large, resulting in the fault not being detected.

B. Results of fault estimation and fault tolerant control

It is noted that Case 1 satisfies the proposed judgement condition 1, hence the FE scheme (69)-(70) in Theorem 2 will be utilized; however, Case 2 does not satisfy the proposed judgement condition 1, therefore the FE scheme (82)-(80) in Theorem 3 will be adopted. The fault and its estimate are shown in Fig. 10 and Fig. 11 for Case 1 and Case 2 respectively. It is clear that the proposed two FE schemes can both achieve good estimation performance. It is noted that for

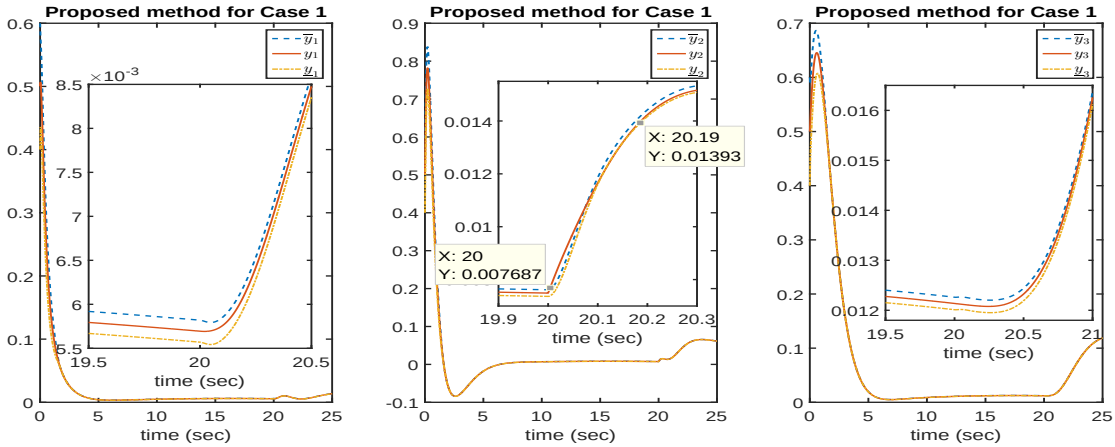

Fig. 6: Outputs $y_i, i = 1,2,3$ and their upper and lower bounds for Case 1 with the proposed IO.

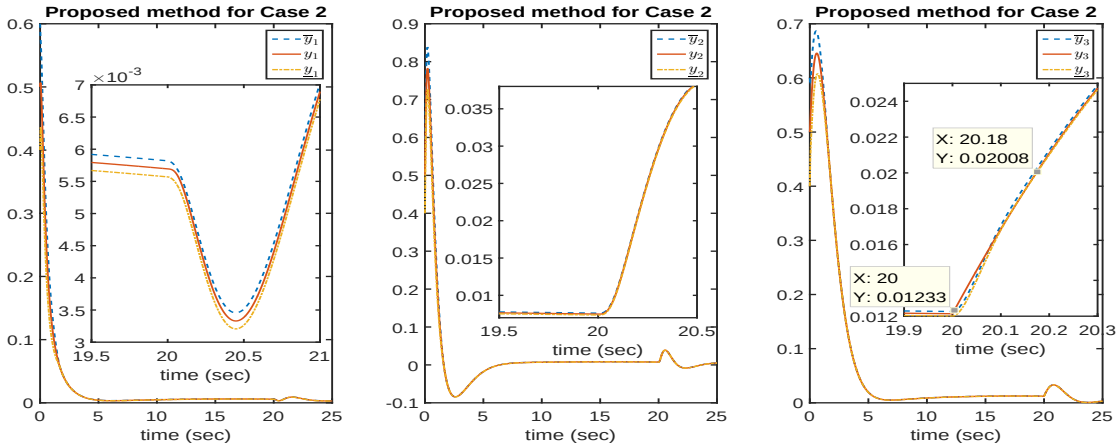

Fig. 7: Outputs $y_i, i = 1,2,3$ and their upper and lower bounds for Case 2 with the proposed IO.

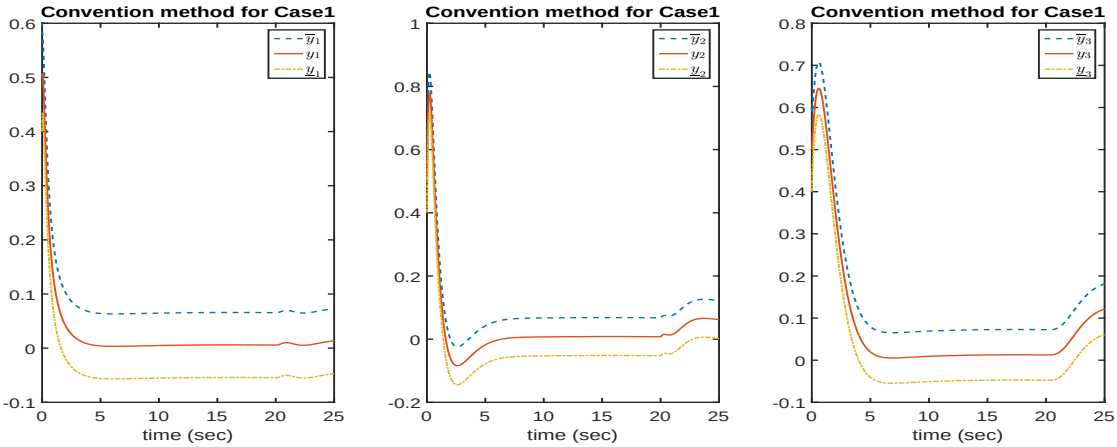

Fig. 8: Outputs $y_i, i = 1,2,3$ and their upper and lower bounds for Case 1 with the conventional IO.

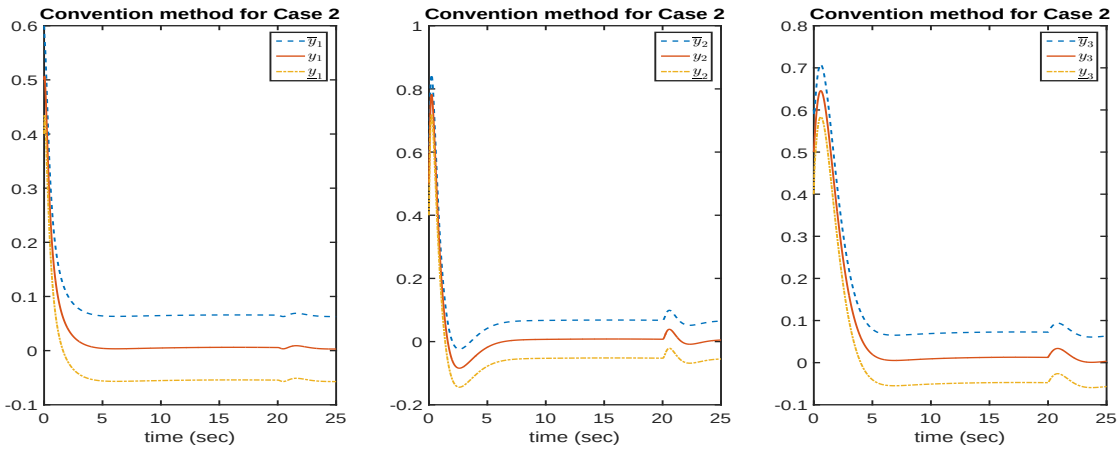

Fig. 9: Outputs $y_i, i = 1,2,3$ and their upper and lower bounds for Case 2 with the conventional IO.

Case 2, the existing FE methods [9, 10] cannot be applicable since the matrix equalities/inequalities are not feasible.

Using the fault estimate, the fault tolerant controller (91) is constructed and applied. The control voltages V_f and V_b, and desired and actual attitude angles for two cases are presented in Fig. 10 and Fig. 11 respectively. Apparently, the proposed FTC scheme (91) can ensure good attitude angle tracking performance.

VI. Conclusion

In this paper, an output feedback active FTC for a 3-DOF helicopter with sensor faults has been developed. We have designed an adaptive IO, which acts not only as state and disturbance estimator but also as FDI observer for the fault location. Next, according to the fault location, a judgment condition is proposed and then FTC based on two different FE schemes is established to ensure the acceptable tracking performance. The proposed disturbance estimation scheme is only suitable for the constant disturbance, and in the future, studies on the estimation of varying disturbance will be conducted.

Acknowledgments

This work was supported by the National Natural Science Foundation of China under Grant 61973197 and Science and Technology Support Plan for Youth Innovation of Colleges and Universities of Shandong Province of China (2021KJ028).

References

[1] X. Zhu, D. Li, "Robust fault estimation for a 3-DOF helicopter considering actuator saturation," *Mechanical Systems and Signal Processing*, vol. 155, no. 107624, 2021.

[2] J. Kang, G. Guo, G. Yang, "Distributed Optimization of Uncertain Multiagent Systems With Disturbances and Actuator Faults via Exosystem Observer-Based Output Regulation," *IEEE Trans. Circuits and Systems I: Regular Papers*, vol. 70, no. 2, pp. 897–909, 2023.

[3] S. Zeghlache, T. Benslimane, A. Bouguerra, "Active fault tolerant control based on interval type-2 fuzzy sliding mode controller and non linear adaptive observer for 3-DOF laboratory helicopter," *ISA transactions*, vol. 71, pp. 280–303, 2017.

[4] T. Wang, M. Lu, X. Zhu, R. Patton, "Aggressive Maneuver Oriented Robust Actuator Fault Estimation of a 3-DOF Helicopter Prototype Considering Measurement Noises," *IEEE-ASME Trans. Mechatronics*, vol. 27, no. 3, pp. 1672–1682, 2022.

[5] J. Lan, R. Patton, X. Zhu, "Integrated fault-tolerant control for a 3-DOF helicopter with actuator faults and saturation," *IET Control Theory & Applications*, vol. 11, no. 14, pp. 2232–2241, 2017.

[6] X. Wang, W. Zhai, X. Zhang, et al., "Enhanced Automotive Sensing Assisted by Joint Communication and Cognitive Sparse MIMO Radar," *IEEE Trans. Aerospace and Electronic Systems*, DOI: 10.1109/TAES.2023.3271614.

[7] W. Zhang, D. Xu, B. Jiang, et al., "Virtual-Sensor-Based Model-Free Adaptive Fault-Tolerant Constrained Control for Discrete-Time Nonlinear Systems," *IEEE Trans. Circuits and Systems I: Regular Papers*, vol. 69, no. 10, pp. 4191–4202, 2022.

[8] Z. Li, H. Liu, B. Zhu, H. Gao, "Robust second-order consensus tracking of multiple 3-DOF laboratory helicopters via output feedback," *IEEE/ASME Trans. Mechatronics*, vol. 20, no. 5, pp. 2538–2549, 2015.

[9] C. Liu, B. Jiang, K. Zhang, S. Ding, "Hierarchical Structure-Based Fault-Tolerant Tracking Control of Multiple 3-DOF Laboratory Helicopters," *IEEE Trans. Systems, Man, and Cybernetics: Systems*, vol. 52, no. 7, pp. 4247–4258, 2022.

[10] C. Liu, B. Jiang, R. Patton, K. Zhang, "Hierarchical structure-based adaptive fault-tolerant consensus control for multiple 3-DOF laboratory helicopters," *Int. J. Adaptive Control and Signal Processing*, vol. 34, no. 8, pp. 992–1012, 2020.

[11] J. Dong, Y. Wu, G. Yang, "A new sensor fault isolation method for TCS fuzzy systems," *IEEE Trans. Cybernetics*,

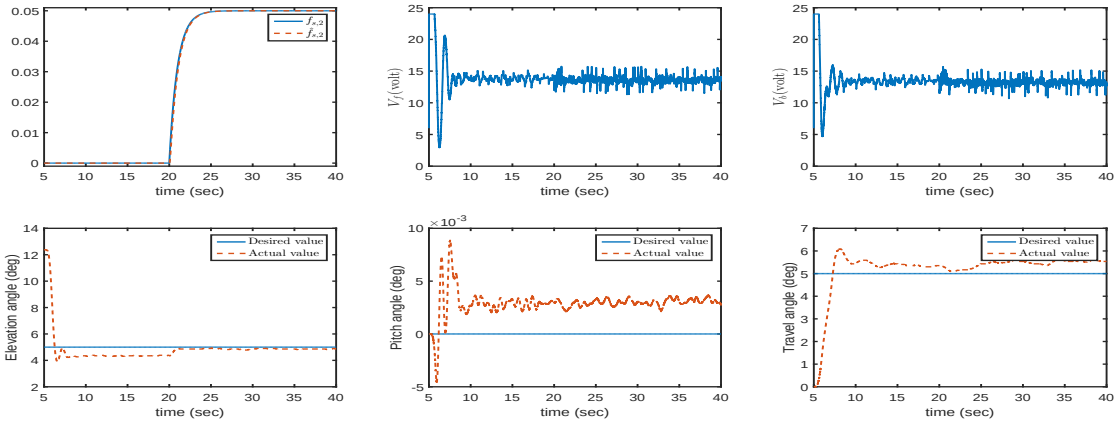

Fig. 10: Fault estimate, control voltages and orientation angles for Case 1.

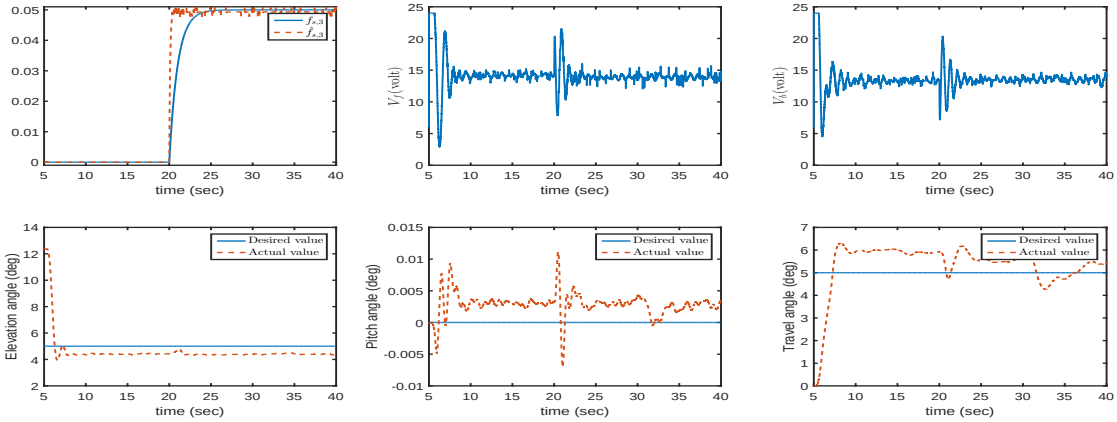

Fig. 11: Fault estimate, control voltages and orientation angles for Case 2.

vol. 47, no. 9, pp. 2437–2447, 2017.

[12] J. Dong, J. Hou, "Output feedback fault-tolerant control by a set-theoretic description of TCS fuzzy systems," *Applied Mathematics and Computation*, vol. 301, pp. 117–134, 2017

[13] N. Ellero, D. Gucik-Derigny, and D. Henry, "Interval observer for Linear Time Invariant (LTI) uncertain systems with state and unknown input estimations," *J. physics: Conference series*, vol. 659, no. 1, IOP Publishing (012023), 2015.

[14] Z. Zhang, and G. Yang, "Distributed fault detection and isolation for multiagent systems: An interval observer approach," *IEEE Trans. Systems, Man, and Cybernetics: Systems*, vol. 50, no. 6, pp. 2220–2230, 2018.

[15] F. Zhu, Y. Tang, Z. Wang, "Interval-Observer-based fault detection and isolation design for TS fuzzy system based on zonotope analysis," *IEEE Trans. Fuzzy Systems*, vol. 30, no. 4, pp. 945–955, 2021.

[16] J. Zhang, and F. Zhu, "On the observer matching condition and unknown input observer design based on the system left-invertibility concept," *Trans. Inst. Measurement and Control*, vol. 40, no. 9, pp. 2887–2900, 2018.

[17] A. R. de Souza, D. Efimov, T. Raissi, "Robust output feedback MPC for LPV systems using interval observers," *IEEE Trans. Automatic Control*, vol. 67, no. 6, pp. 3188–3195, 2021.

[18] X. Wang, C. Tan, "Output Feedback Active Fault Tolerant Control for a 3-DOF Laboratory Helicopter with Sensor Fault," *IEEE Trans. Automation Science and Engineering*, DOI:10.1109/TASE.2023.3267132.

[19] 3-DOF Helicopter Reference Manual. Quanser Consulting Inc. 2006.

[20] D. Zhao, M. Polycarpou, "Distributed Fault Accommodation of Multiple Sensor Faults for a Class of Nonlinear Interconnected Systems," *IEEE Trans. Automatic Control*, vol. 67, no. 4, pp. 2092–2099, 2022.

[21] S. Waslander, and C. Wang, "Wind disturbance estimation and rejection for quadrotor position control," in *Proc. AIAA Infotech Aerospace conference*, Seattle, Washington, USA, 2209, no. AIAA 2009-1983.

[22] N. Ellero, D. Derigny, D. Henry, "An unknown input interval observer for LPV systems under L_2-gain and L_∞-gain criteria," *Automatica*, vol. 103, pp. 294–301, 2019.

[23] La Salle, P. Joseph, "An invariant principle in the theory

of stability," No. NASA-CR-74165, 1966.
[24] K. Zhao, R. Zhou, J. She, et al, "Demagnetization-Fault Reconstruction and Tolerant-Control for PMSM Using Improved SMO-Based Equivalent-Input-Disturbance Approach," *IEEE-ASME Trans. Mechatronics*, vol. 27, no. 2, pp. 701–712, 2022.
[25] Y. Li, Z. Ma, S. Tong, "Adaptive fuzzy fault-tolerant control of nontriangular structure nonlinear systems with error constraint," *IEEE Trans. Fuzzy Systems*, vol. 26, no. 4, pp. 2062–2074, 2017.
[26] J. Lan, and R. J. Patton, "Integrated fault estimation and fault-tolerant control for uncertain Lipschitz nonlinear systems," *Int. J. Robust and Nonlinear Control*, vol. 27, no. 5, pp. 761–780, 2017.

Xianghua Wang received the B.E. degree in Automation from Northwestern Polytechnical University, Xi'an, China, in 2010 and the Ph.D. degree in Mechanical System and Control from Peking University, Beijing, China, in 2015. She is currently an associate professor at Beijing University of Posts and Telecommunications. Her current research interests include fault diagnosis, fault tolerant control, guidance and control. She authored or co-authored 1 book and more than 50 papers.

YouqingWang received the B.S. degree in Mathematics from Shandong University, Jinan, China, in 2003, and Ph.D. degree in Control Science and Engineering from Tsinghua University, Beijing, China, in 2008. He is currently a Professor at Beijing University of Chemical Technology, Beijing, China. His research interests include fault diagnosis, fault-tolerant control, state monitoring, and iterative learning control for chemical and biomedical processes. Dr. Wang was a recipient of several research awards, including the NSFC Excellent Young Scientists Fund, the Journal of Process Control Survey Paper Prize and ADCHEM2015 Young Author Prize.

Ziye Zhang received the B.S. degree in mathematics from Yantai University, Yantai, China, in 2002, the M.S. degree in mathematics from Lanzhou University, Lanzhou, China, in 2005, and the Ph.D. degree from the Institute of Complexity Science, Qingdao University, Qingdao, China, in 2015. She is currently an associate professor at Shandong University of Science and Technology. Her current research interests include systems analysis, fuzzy control, filter design and neural networks.

Xiangrong Wang received the the B.E and M.E degrees in electrical engineering from Nanjing University of Science and Technology, China, in 2009 and 2011, respectively, and the Ph.D. degree in signal processing from University of New South Wales, Australia in 2015. She is currently an associate professor at Beihang University. Her research interest includes array signal processing, parameter estimation, time-frequency analysis and spectrum sharing. She authored or co-authored 1 book, 1 book chapter and more than 60 papers.

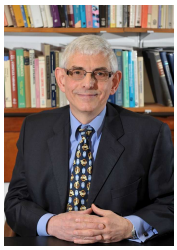

Ron Patton (Life Fellow, IEEE) is Professor of Control and Intelligent Systems Engineering (C&ISE) in the School of Engineering, University of Hull. His research is involved with the development of robust methods of fault detection and diagnosis (FDD) for control systems and fault tolerant control (FTC) to enhance the reliability of computer control systems. His application interest is the development and design of control and estimation methods for flight systems and to enhance energy efficiency, fault tolerance and reliability of renewable energy systems in offshore wind, and wave energy conversion. He is widely published with an H-index of H-68.